

THE DEVELOPMENT OF Pt/WO_x/Al₂O₃ FOR 1,3-PROPANEDIOL PRODUCTION FROM
GLYCEROL



A Thesis Submitted in Partial Fulfillment of the Requirements
for the Degree of Master of Engineering in Chemical Engineering

Department of Chemical Engineering

Faculty of Engineering

Chulalongkorn University

Academic Year 2018

Copyright of Chulalongkorn University

การพัฒนาตัวเร่งปฏิกิริยา Pt/WO_x/Al₂O₃สำหรับการผลิต 1,3-โพรเพนไดออลจากกลีเซอรอล



วิทยานิพนธ์นี้เป็นส่วนหนึ่งของการศึกษาตามหลักสูตรปริญญาวิทยาศาสตรมหาบัณฑิต

สาขาวิชาวิศวกรรมเคมี ภาควิชาวิศวกรรมเคมี

คณะวิศวกรรมศาสตร์ จุฬาลงกรณ์มหาวิทยาลัย

ปีการศึกษา 2561

ลิขสิทธิ์ของจุฬาลงกรณ์มหาวิทยาลัย

Thesis Title THE DEVELOPMENT OF Pt/WO_x/Al₂O₃ FOR 1,3-
PROPANEDIOL PRODUCTION FROM GLYCEROL
By Mr. Parama Uttraporn
Field of Study Chemical Engineering
Thesis Advisor Professor PIYASAN PRASERTHDAM, Dr.Ing.
Thesis Co Advisor Junjuda Unruangsri, Ph.D.

Accepted by the Faculty of Engineering, Chulalongkorn University in Partial
Fulfillment of the Requirement for the Master of Engineering

..... Dean of the Faculty of Engineering
(Professor SUPOT TEACHAVORASINSKUN, D.Eng.)

THESIS COMMITTEE

..... Chairman
(Akawat Sirisuk, Ph.D.)

..... Thesis Advisor
(Professor PIYASAN PRASERTHDAM, Dr.Ing.)

..... Thesis Co-Advisor
(Junjuda Unruangsri, Ph.D.)

..... Examiner
(Assistant Professor Pattaraporn Kim, Ph.D.)

..... External Examiner
(Assistant Professor Okorn Mekasuwandumrong, D.Eng.)

ปรมะ อุตสาหกรรม : การพัฒนาตัวเร่งปฏิกิริยา Pt/WO_x/Al₂O₃สำหรับการผลิต 1,3-โพรเพนไดออลจากกลีเซอรอล. (THE DEVELOPMENT OF Pt/WO_x/Al₂O₃ FOR 1,3-PROPANEDIOL PRODUCTION FROM GLYCEROL) อ.ที่ปรึกษาหลัก : ศ. ดร.ปิยะสาร ประเสริฐธรรม, อ.ที่ปรึกษาร่วม : ดร.จัญจดา อุ๋นเรืองศรี

ในงานวิจัยนี้ศึกษาปฏิกิริยาไฮโดรจีโนไลซิสของกลีเซอรอล โดยการเปรียบเทียบความต่างของตัวรองรับระหว่างโบฮีไมต์และแกมมาอะลูมินา ใช้ตัวเร่งปฏิกิริยาคือแพลตตินัม/ทังสเทน/โบฮีไมต์ และ แพลตตินัม/ทังสเทน/แกมมาอะลูมินา สังเคราะห์โดยวิธีการเคลือบฝังตัวเร่งปฏิกิริยาแบบเปียก เพื่อศึกษาสมบัติของตัวเร่งปฏิกิริยา จะทำการวิเคราะห์ด้วยเทคนิคต่างๆ เช่น การเลี้ยวเบนรังสี เทคนิคอินฟราเรดสเปกโตรสโคปีด้วยไพริดีน และ เทคนิคการโปรแกรมอุณหภูมิเพื่อทดสอบการคายซัพของแอมโมเนีย เป็นต้น จากผลการวิจัยพบว่า ค่าร้อยละการเปลี่ยนแปลงและการเลือกเกิดบนตัวรองรับแกมมาอะลูมินามีค่าสูงกว่าตัวรองรับโบฮีไมต์เนื่องจากมีปริมาณของกรดบรอนสเตดและตำแหน่งที่ว่างไว้มากกว่า นอกจากนี้ยังได้ทำการศึกษาผลของความดันก๊าซไฮโดรเจน การเพิ่มปริมาณแพลตตินัม และปริมาณทังสเทนบนตัวรองรับแกมมาอะลูมินาด้วยเช่นกัน นอกจากนี้งานวิจัยนี้ได้ศึกษาผลของตัวเร่งปฏิกิริยาหลังจากนำตัวเร่งปฏิกิริยาไปผ่านกระบวนการรีดักชันที่อุณหภูมิ 300 องศาเซลเซียสต่อค่าร้อยละการเปลี่ยนแปลงและค่าการเลือกเกิดจำเพาะของ 1,3-โพรเพนไดออล พบว่าตัวเร่งปฏิกิริยาที่ผ่านกระบวนการรีดักชัน จะมีผลทำให้ปริมาณของกรดบรอนสเตดและตำแหน่งที่ว่างไว้ออกฤทธิ์ลดลงส่งผลถึงค่าร้อยละการเปลี่ยนแปลงของกลีเซอรอลและค่าการเลือกเกิดของ 1,3-โพรเพนไดออลลดลงเช่นกัน ดังนั้นปริมาณกรดบรอนสเตดและตำแหน่งความว่างไว้ออกฤทธิ์จึงมีความสำคัญต่อการเลือกเกิด 1,3-โพรเพนไดออลของปฏิกิริยาไฮโดรจีโนไลซิส

สาขาวิชา วิศวกรรมเคมี

ปีการศึกษา 2561

ลายมือชื่อนิสิต

ลายมือชื่อ อ.ที่ปรึกษาหลัก

ลายมือชื่อ อ.ที่ปรึกษาร่วม

5970238821 : MAJOR CHEMICAL ENGINEERING

KEYWORD: hydrogenolysis, glycerol, Platinum, Tungsten oxide

Parama Uttraporn : THE DEVELOPMENT OF Pt/WO_x/Al₂O₃ FOR 1,3-PROPANEDIOL PRODUCTION FROM GLYCEROL. Advisor: Prof. PIYASAN PRASERTHDAM, Dr.Ing. Co-advisor: Junjuda Unruangsri, Ph.D.

In this work, the researcher studied the hydrogenolysis of glycerol to 1,3-propanediol, by compared the catalytic activity between ALOOH (boehmite) and g-Al₂O₃. The catalysts were prepared by wet impregnation method. To investigate the properties, catalysts were characterized by XRD, XPS, BET, H₂-TPR, H₂-TPD, H₂-TPR, SEM-EDX, Py-IR, NH₃-IR, and XAS. The type of support showed to be of significance in deciding the activity and the selectivity to 1,3-propanediol. It was found that 2%Pt/WO_x/g-Al₂O₃ gave higher activity and selectivity of 1,3-propanediol, which due to a large amount of active site and Brønsted acid site in the catalyst. The effects of H₂ pressure, %Pt loading and WO_x content were also examined. Furthermore, the researcher has investigated the effect of pretreated catalyst to catalytic activity. The reduced catalysts showed the decline in Pt dispersion and Brønsted acid site led to the decreasing of glycerol conversion and selectivity of 1,3-propanediol. So the concentration of Brønsted acid sites presented as a main to the selective production of 1,3-propanediol from glycerol hydrogenolysis.

Field of Study: Chemical Engineering

Academic Year: 2018

Student's Signature

Advisor's Signature

Co-advisor's Signature

ACKNOWLEDGEMENTS

I was grateful to express my sincere gratitude to my thesis advisor, Professor Dr. Piyasan Praserthdam and Dr. Junjuda Unruangsri my co-advisor to give advice about my thesis, guidance, suggestion, and supported during experimentation and discussion in order to achieve my thesis.

In addition, I will also be grateful to Dr. Akawat Sirisuk represented as the leader. Including, Asst. Prof. Dr. Pattaraporn Kim and Asst. Prof. Dr. Okorn Mekasuwandumrong acted as the thesis committee for a good suggestion. I would thank you for members and scientist in Center of Excellence on Catalysis and Catalytic Reaction Engineering of Chemical Engineering Faculty of Engineering Chulalongkorn University who guidance for equipment and preparation.

I gratefully thank the Government Budget for financial support. This research is funded by Chulalongkorn University.

I would like to thank my friends for any helping and be enduring to me. I appreciate thanking my family for supporting me in successful writing this thesis.



Parama Uttraporn

TABLE OF CONTENTS

	Page
ABSTRACT (THAI).....	iii
ABSTRACT (ENGLISH).....	iv
ACKNOWLEDGEMENTS.....	v
TABLE OF CONTENTS.....	vi
LIST OF FIGURES.....	ix
LIST OF TABLES.....	xii
LIST OF SCHEMES.....	xiii
CHAPTER I INTRODUCTION.....	14
1.1 Introduction.....	14
1.2 Objective.....	17
1.3 The scope of the research.....	17
1.4 Research methodology.....	18
CHAPTER II BACKGROUND AND LITERATURE REVIEWS.....	19
2.1 Glycerol.....	19
2.2 Hydrogenolysis reaction of glycerol to 1,3-PD.....	24
2.3 Catalyst and Literature review.....	26
CHAPTER III EXPERIMENTAL.....	33
3.1 General.....	33
3.2 Catalyst Preparation.....	33
3.2.1 $WO_x/\gamma-Al_2O_3$	33
3.2.2 $x\%Pt/WO_x/\gamma-Al_2O_3$	33

3.2.3 x%Pt/WO _x /Al ₂ O ₃ reduced catalyst	34
3.3 Typical Hydrogenolysis Reaction	34
3.4 Catalyst Characterization.....	35
3.4.1 X-ray diffraction (XRD)	36
3.4.2 X-ray photoelectron spectroscopy (XPS).....	36
3.4.3 CO-Pulse Chemisorption.....	36
3.4.4 N ₂ -physisorption.....	36
3.4.5 Scanning electron microscope (SEM).....	37
3.4.6 X-ray absorption spectroscopy (XAS).....	37
3.4.7 NH ₃ -TPD	37
3.4.8 IR spectra of pyridine adsorption.....	37
3.4.9 IR spectra of ammonia adsorption.....	38
3.4.10 Temperature-programmed desorption of hydrogen (H ₂ -TPD).....	38
3.4.11 Temperature-programmed reduction of hydrogen (H ₂ -TPR)	39
CHAPTER IV RESULTS AND DISCUSSION	40
4.1 Effect of calcination temperature to catalytic activity.....	40
4.1.1 X-ray diffraction (XRD)	40
4.1.2 N ₂ -physisorption.....	42
4.1.3 IR spectra of ammonia adsorption.....	43
4.1.4 NH ₃ -Temperature Programed Desorption.....	45
4.2 Effect of Hydrogen pressure to 2%Pt/WO _x /γ-Al ₂ O ₃	47
4.3 Effect of %Pt loading to catalytic activity	49
4.3.1 CO chemisorption.....	49
4.3.2 X-ray diffraction (XRD)	50

4.3.3 NH ₃ -Temperature Programed Desorption.....	51
4.3.4 IR spectra of ammonia adsorption	52
4.4 Effect of tungsten oxide content to catalytic activity	56
4.4.1 IR spectra of pyridine adsorption.....	56
4.5 Effect of pretreatment on catalytic activity.....	60
4.5.1 IR spectra of pyridine adsorption.....	61
4.5.2 Temperature-programmed reduction of hydrogen (H ₂ -TPR).....	61
4.5.3 Temperature-programmed desorption of hydrogen (H ₂ -TPD)	62
4.5.4 X-ray absorption spectroscopy (XAS).....	63
CHAPTER IV CONCLUSION AND RECOMMENDATIONS	69
5.1 Conclusion	69
5.2 Recommendation	69
REFERENCES	70
APPENDIX.....	78
APPENDIX A CALIBRATION CURVES	79
APPENDIX B CALCULATIONS.....	82
APPENDIX C CALCULATION FOR CO CHEMISORPTION	84
APPENDIX D SEM IMAGES AND EDX MAPS FOR Pt/WO _x /γ-Al ₂ O ₃ CATALYSTS	85
APPENDIX E XPS PHOTOEMISSION FOR 2%Pt/WO _x /AlOOH and 2%Pt/WO _x /γ-Al ₂ O ₃	86
VITA.....	87

LIST OF FIGURES

	Page
Figure 1.1 Production of biodiesel in the world in 2015.....	15
Figure 1.2 Main raw material for the production of biodiesel.....	15
Figure 2.1 Molecular of glycerol structure	19
Figure 2.2 Application of glycerol in industry.....	21
Figure 2.3 Routes for the glycerol conversion process.....	22
Figure 2.4 Byproduct from hydrogenolysis to 1,3-propanediol process.....	25
Figure 2.5 Proposed reaction mechanism for the conversion of glycerol to..... propylene glycol	28
Figure 2.6 Model structures of the transition states of the hydride attack..... to the adsorbed substrate in the glycerol hydrogenolysis	29
Figure 3.1 Experimental equipment for hydrogenolysis of glycerol reaction.....	35
Figure 4.1 XRD patterns of a) 2%Pt/WO _x /boehmite b) 2%Pt/WO _x /γ-Al ₂ O ₃ and c) WO _x /γ-Al ₂ O ₃	40
Figure 4.2 SEM images of catalysts (top) 2%Pt/WO _x /γ-Al ₂ O ₃ (bottom)..... 2%Pt/WO _x /AlOOH	42
Figure 4.3 FTIR of adsorbed NH ₃ on fresh 2%Pt/WO _x /AlOOH..... (calcined at 800°C) and fresh 2%Pt/WO _x /γ-Al ₂ O ₃ (calcined at 900°C) catalysts.	44

Figure 4.4 NH ₃ -TPD profiles of a) 2%Pt/WO _x /AlOOH and.....	45
b) 2%Pt/WO _x /γ-Al ₂ O ₃ catalysts.	
Figure 4.5 Glycerol conversion and product selectivity obtained.....	46
from hydrogenolysis of glycerol over different catalysts.	
Figure 4.6 Effect of H ₂ pressure on glycerol hydrogenolysis over.....	48
2%Pt/WO _x /γ-Al ₂ O ₃ catalyst a) glycerol conversion and b) product selectivity	
Figure 4.7 XRD patterns of the a) 2%Pt/WO _x /γ-Al ₂ O ₃ , b) 5%Pt/WO _x /γ-Al ₂ O ₃ ,.....	50
and c) 8%Pt/WO _x /γ-Al ₂ O ₃ catalysts.	
Figure 4.8 TPD of ammonia profiles of various %Pt loading supported on.....	52
WO _x /γ-Al ₂ O ₃ catalysts.	
Figure 4.9 FTIR of adsorbed NH ₃ on fresh 2%Pt/WO _x /Al ₂ O ₃ , 5%Pt/WO _x /γ-Al ₂ O ₃ ,.....	53
and 8%Pt/WO _x /γ-Al ₂ O ₃ catalysts.	
Figure 4.10 Effect of %Pt content on Glycerol Hydrogenolysis.....	54
to 1,3-PDO.	
Figure 4.11 FTIR spectra of pyridine adsorption of 2%Pt/Al ₂ O ₃ and.....	57
2%Pt/WO _x /Al ₂ O ₃ with different tungsten loading catalysts	
Figure 4.12 FTIR spectra of pyridine adsorption of a) 2%Pt/WO _x /Al ₂ O ₃ ,.....	61
b) 5%Pt/WO _x /Al ₂ O ₃ , and c) 2%Pt/WO _x /Al ₂ O ₃ pretreat with H ₂ at 300 °C and	
2%Pt/WO _x /Al ₂ O ₃ pretreat with H ₂ at 300 °C catalysts	

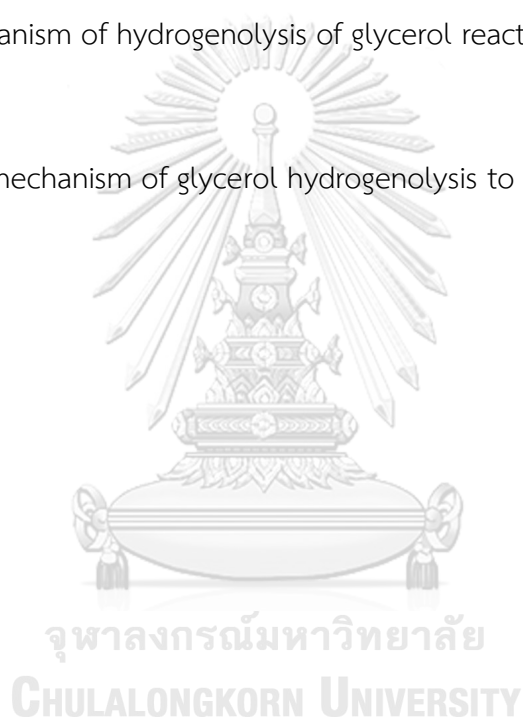
Figure 4.13 H ₂ -TPR profiles only observed on	62
a). 2%Pt/WO _x /γ-Al ₂ O ₃ and b). 5%Pt/WO _x /γ-Al ₂ O ₃ catalysts	
Figure 4.14 H ₂ -TPR profiles only observed on 2%Pt/WO _x /γ-Al ₂ O ₃ and.....	63
5%Pt/WO _x /γ-Al ₂ O ₃ catalysts	
Figure 4.15 Pt L3-edge XANES spectra of 2%Pt/WO _x /γ-Al ₂ O ₃ catalysts.....	64
Figure 4.16 The K ³ -weighted Fourier transforms spectra from EXAFS of catalysts.....	65
Figure 4.17 W L3-edge XANES spectra of catalysts.....	66
Figure A.1 Calibration curve of Glycerol.....	72
Figure A.2 Calibration curve of 1,3-propanediol.....	73
Figure A.3 Calibration curve of 1,2-propanediol.....	73
Figure A.4 Calibration curve of Ethanol.....	74
Figure A.5 Calibration curve of n-propanol.....	74
Figure D.1 SEM-EDX for Pt images of (a,b) 5%Pt/WO _x /γ-Al ₂ O ₃ and.....	78
(c,d) 5%Pt/WO _x /γ-Al ₂ O ₃	
Figure E.1 W 4f XPS spectra of a) 2%Pt/WO _x /ALOOH fresh catalyst,.....	79
b) 2%Pt/WO _x /ALOOH used, c) 2%Pt/WO _x /ALOOH reduced, d) 2%Pt/WO _x /γ-Al ₂ O ₃	
fresh, e) 2%Pt/WO _x /γ-Al ₂ O ₃ used, f) 2%Pt/WO _x /γ-Al ₂ O ₃ reduced.	

LIST OF TABLES

	Page
Table 2.1 Chemical and physical properties of glycerol.....	20
Table 3.1 Operating conditions for gas chromatography.....	35
Table 4.1 N ₂ -Physisorption, CO-Chemisorption, acidities a catalytic.....	43
activities results of the impregnated catalysts.	
Table 4.2 The amounts of Brønsted and Lewis acid sites over the catalysts.....	44
determined from the in situ DRIFTS of adsorbed NH ₃	
Table 4.3 Physicochemical properties, acidities of Pt/WO _x /γ-Al ₂ O ₃ with.....	49
different %Pt loading content and activity result obtained after 12 h, 140 °C, and 0.5 MPa pressure.	
Table 4.4 The amounts of Brønsted and Lewis acid sites over the catalysts.....	54
with difference %Pt loading determined from the in situ DRIFTS of adsorbed NH ₃	
Table 4.5 Summarized the textural properties, acidities and the catalytic activity.....	58
for 2%Pt/WO _x /γ-Al ₂ O ₃ with different tungsten content catalysts.	
Table 4.6 Catalytic performance of glycerol hydrogenolysis over.....	68
x%Pt/WO _x /γ-Al ₂ O ₃ pretreated and non-pretreated catalysts	

LIST OF SCHEMES

	Page
Scheme 1.1 Formation of glycerol by A) hydrolysis, B) saponification.....16 and C) biodiesel processes	
Scheme 2.1 The pathways of glycerol to propanediol by hydrogenolysis.....25 reaction	
Scheme 2.2 Mechanism of hydrogenolysis of glycerol reaction with.....30 Pt/WO ₃ catalyst	
Scheme 2.3 The mechanism of glycerol hydrogenolysis to 1,3-propanediol.....31 over Pt-ALO _x /WO _x	



CHAPTER I

INTRODUCTION

1.1 Introduction

Nowadays manufacturing has the procedure to develop the biodiesel product from natural for diminished the introduction of petrochemical, which the price is unstable. The sustainable biodiesel is option. It has attracted huge investment in both industrial and academics. Biodiesel is generated from distinct sustainable sources for example vegetable oil and fat of animal, used cooking oil, and etc.

The renewable biodiesel product in worldwide has been increasing in the past few years. In 2016 over 30.8 Mm³ biodiesel were made, giving an increase in production of 7.5 % from 2015. The main producers of biodiesel were United States (5.5 Mm³ per annum), Germany (4.0 Mm³ per annum), Indonesia (3.3 Mm³ per annum) and Argentina (3.1 Mm³ per annum) (Figure 1.1). In 2016, all of the countries in Europe produced 10.7 Mm³. This is equal to 34.7 % of global biodiesel production[1]. The raw material used in biodiesel is diverse, for example, rapeseed, soybean, and palm, of which are the major materials for bioenergy used to produce diesel fuel in Europe, USA, Brazil as well as Argentina and Asia respectively (Figure 1.2).

OECD FAO Agricultural Outlook reported that biodiesel production is estimated to grow around 4.5 % per year and up to 41 Mm³ in 2022. In the near future, the European Union is expected to be the main manufacturer to produce and utilize biodiesel. Meanwhile, other countries for example the United States, Argentina, Brazil, including Thailand and Indonesia are also proclaimed to continue their market leadership in producing biodiesel products [2].

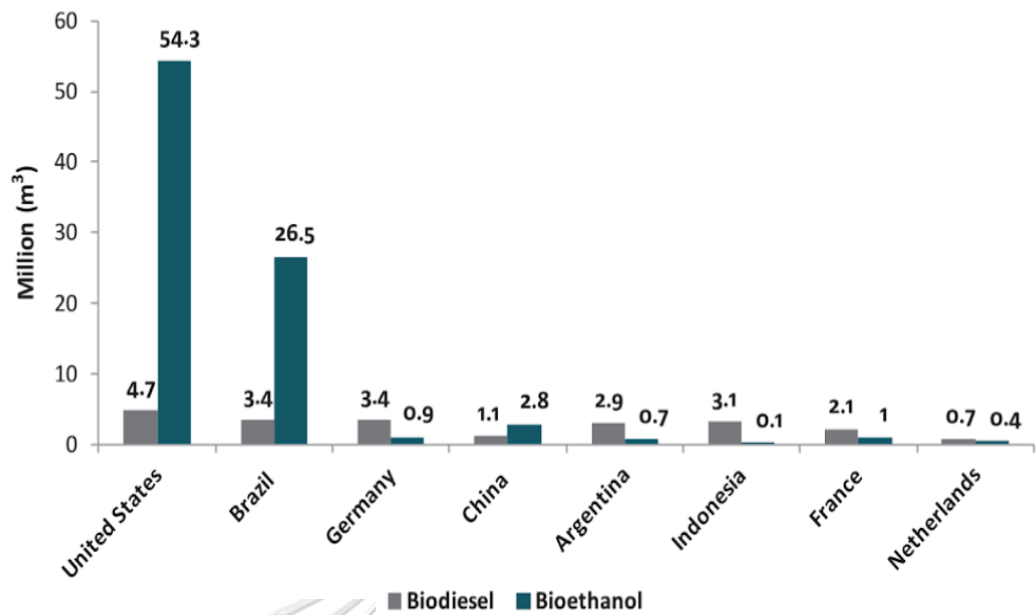


Figure 1.1 Production of biodiesel in the world in 2015 (source: Brazilian Energy Research Enterprise, 2015) [3].

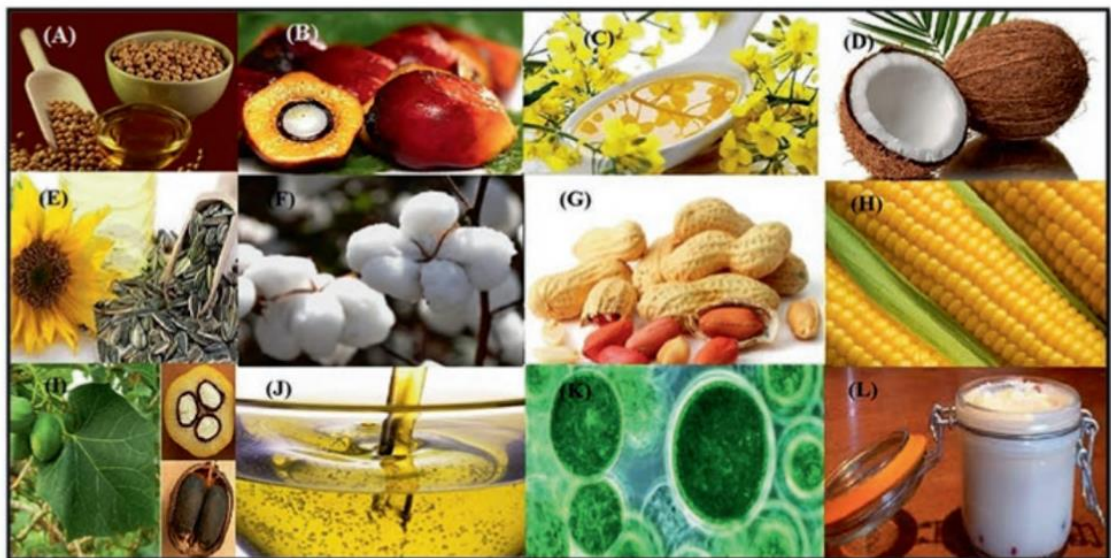
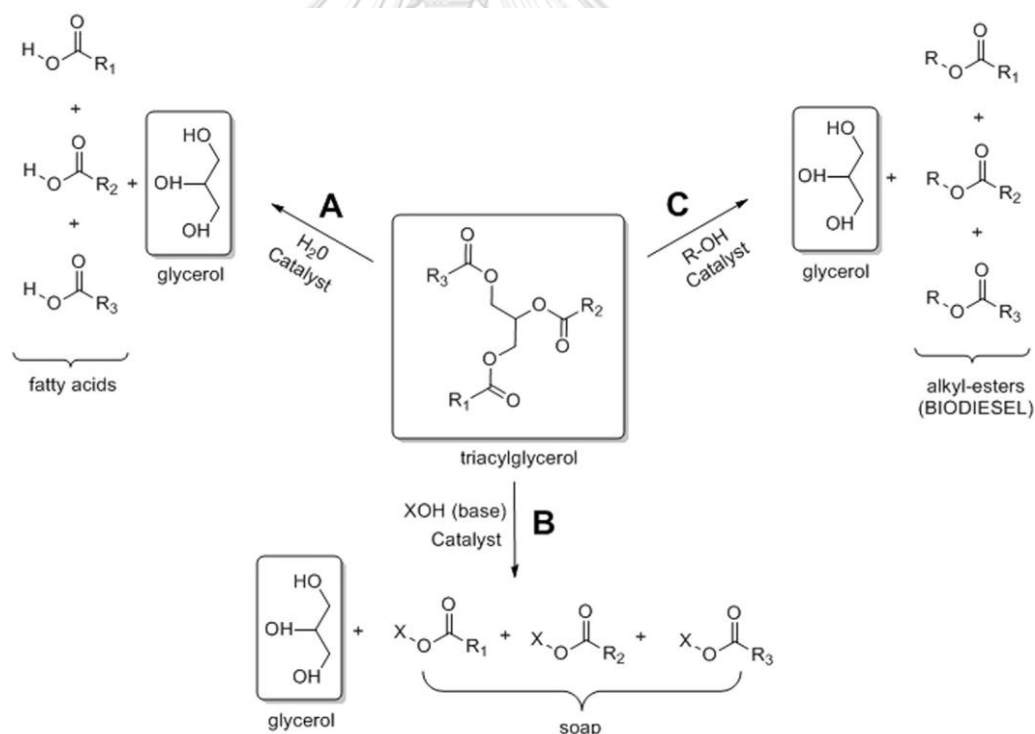


Figure 1.2 Main raw material for the production of biodiesel: (a) soybean, (b) palm, (c) rapeseed, (d) coconut, (e) sunflower, (f) cotton, (g) peanut, (h) corn, (i) *jatropha curcus*, (j) use cooking oil, (k) algae, (l) tallow [4].

Typically, biodiesel obtained from the industrial trans-esterification procedure of fat and oil (triglyceride). It contains of methyl ester (90%) and glycerol (10%). Concerning, number of glycerol were generated in the process of biodiesel. The trans-esterification reaction of triglyceride produced product at the ratio of biodiesel to glycerol is 10:1 for every 1 m³ of biodiesel, so 0.1 m³ of crude glycerol is obtained [5]. Such as in 2015, global production of biodiesel is 30 Mm³ therefor the product of glycerol is over 300000 m³. If the process of biodiesel carried on, it will cause the excess of glycerol production. Therefore the finding new way to produce valuable production from glycerol is very important. Basically, glycerol could produce from the saponification method and hydrolysis reaction as well (Scheme 1 show pathways to produce glycerol)



Scheme 1.1 Formation of glycerol by hydrolysis (A), saponification (B) and biodiesel processes (C) [6].

1.2 Objective

To study effect of pretreated and non-pretreated for hydrogenlysis of glycerol to 1,3-propanediol.

1.3 The scope of the research

The detail of scope research is given below.

1.3.1. The preparation of all catalysts by wet impregnation method.

1.3.2. Synthesis of 2%Pt/WO_x/AlOOH and 2%Pt/WO_x/γ-Al₂O₃

1.3.3. Studied effect of H₂-pressure.

1.3.4. Studied effect of %Pt and %WO_x with different loading.

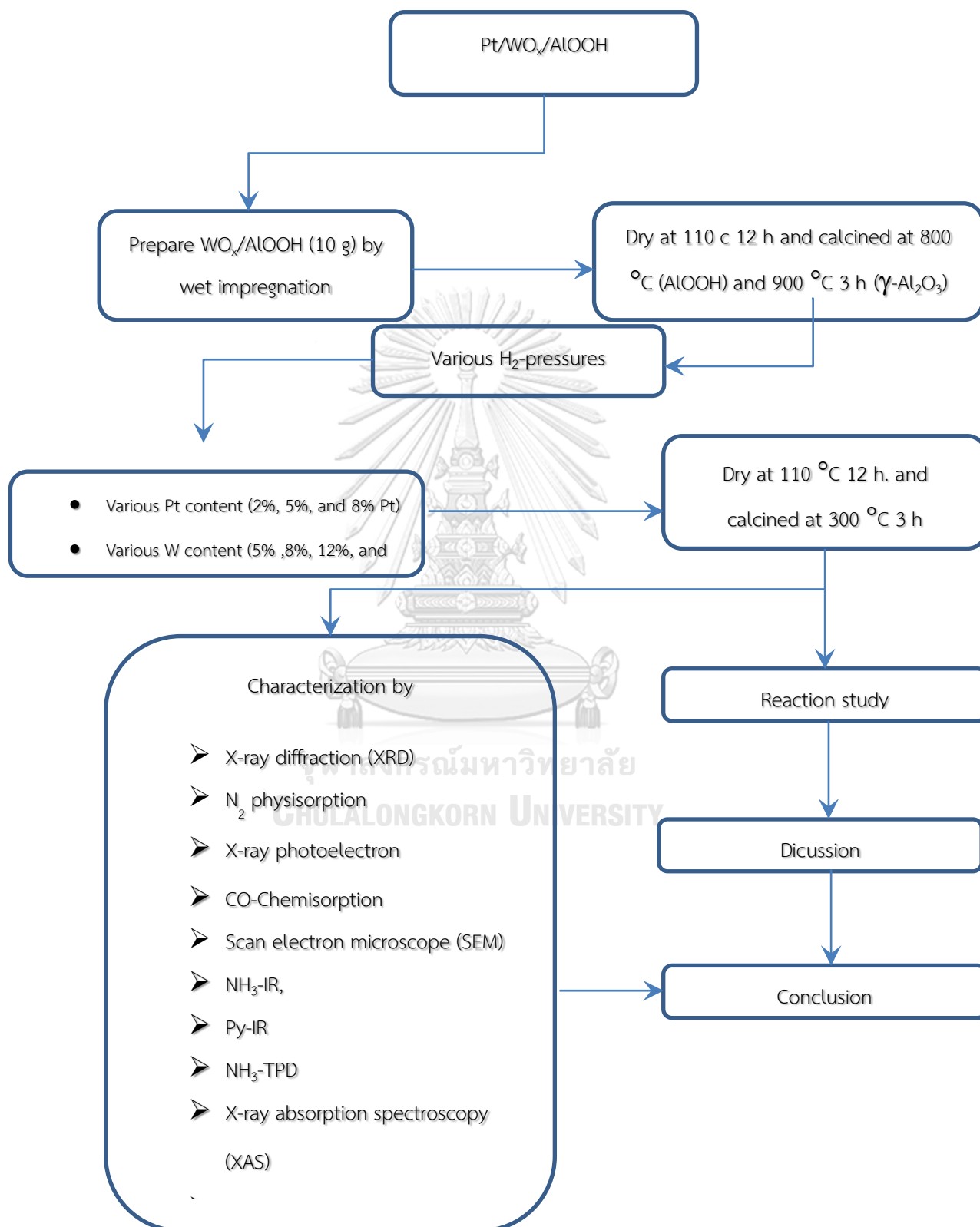
1.3.5. Studied effect of pretreated and non-pretreated catalyst.

1.3.6. The product of the reaction was investigated by GC-FID

1.3.7. Characterization of the catalyst by using various techniques:

- X-ray diffraction (XRD)
- N₂ physisorption
- X-ray photoelectron spectroscopy (XPS)
- IR spectra of ammonia adsorption
- IR spectra of pyridine adsorption
- NH₃-temperature programmed desorption
- Scan electron microscope (SEM)
- CO Chemisorption
- X-ray absorption spectroscopy (XAS)
- Temperature-programmed reduction of hydrogen (H₂-TPR)
- Temperature-programmed desorption of hydrogen (H₂-TPD)

1.4 Research methodology



CHAPTER II

BACKGROUND AND LITERATURE REVIEWS

This section will provide information of principle and mechanism of Hydrogenolysis reaction, properties of catalyst and explain the literature for this work. The detail is explained below:

2.1 Glycerol

Glycerol is a chemical compound. It has uncomplicated formula $C_3H_8O_3$ that contained of the tri-alcohol. IUPAC name of glycerol is a propandiol-1,2,3-triol. It is still well-known by many commercial names as glycerine. Glycerol is colorless, odorless, organic compound, viscous liquid and sweets taste. The molecular of glycerol structure show in Fig 2.1, the pure glycerol consists of three hydroxyl groups that are accountable for the ability to dissolve in water and hygroscopic nature. The boiling point, flash point, and melting point of glycerol is $290^{\circ}C$, $177^{\circ}C$, and $18^{\circ}C$ respectively [7, 8]. Table 2.1 shows the textural and characteristic of glycerol, which is important to apply in the industry.

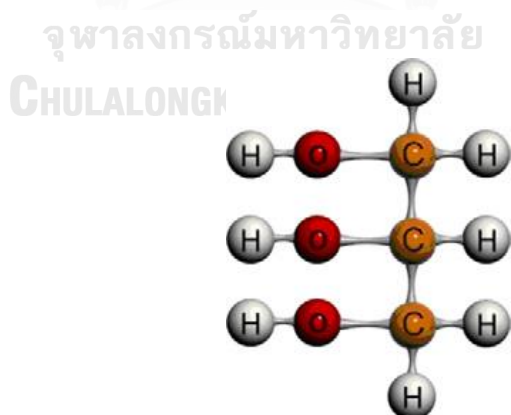


Figure 2.1 Molecular of glycerol structure

Table 2.1 Chemical and physical properties of glycerol [7].

Properties	Valaues	
Chemical formula	CH ₂ -OH-CHOH-CH ₂ -OH	
Formula weight	92.09	
From and colour	Colourless and liquid	
Specific gravity	1.260 ^{50/4}	
Melting point	17.9 °C	
Boiling point	292 °C	
Solubility in 100 part		
• water	Infinitely	
• Alcohol	Infinitely	
• Ether	Insoluble	
Vapor pressure in 760 mmHg	290 °C	
Heat of fusion at 18.07 °C	47.49 cal/g	
Viscosity liquid glycerol		
• 100 %	10 cP	
• 50 %	25 cP	
Specific heat glycerol in aqueous solution (mol%)	15 °C (cal/g °C)	30 °C (cal/g °C)
2.12	0.961	0.96
4.66	0.929	0.924
11.5	0.851	0.841
22.7	0.765	0.758
43.9	0.670	0.672
100	0.555	0.576

Glycerol is a beneficial byproduct because it used for various functions for the industry. Previously, the applications of glycerol have more than two thousand diverse using, particularly in drugs, food and treatment [9]. (Figure. 2.2) Glycerol is a

harmless, edible to eat, and biodegradation of the material, so, glycerol will help essential natural the new products. Glycerol is mostly apply in the manufacturing of pharmaceutical for the objective of pill dissolve, giving the humidity in drugs and improving the liquid pills viscosity and it is also use in ear infection medicines for a carrier of antibiotics, antiseptics, and plastic for medication [10]. Glycerol is an excellent of chemical solvent such as tannins, phenol , bromine, iodine, mercury chloride, and alkaloids [11]. In addition, glycerol was used for personal treatment, mostly use to giving lubrication, developing smoothness, and also use as a moistener in many skin care production [10]. Accordingly, all of the application insufficiency to manage the extra of glycerol in worldwide, thus, the advance production is needed to eliminate the excess glycerol.

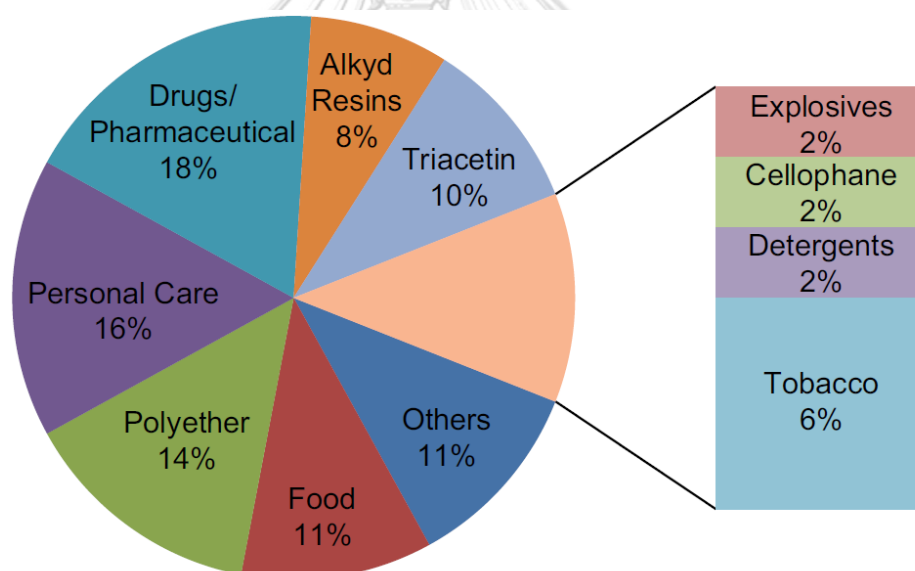


Figure 2.2 Application of glycerol in the industry [12].

Glycerol is the main product induced from the triglyceride industry, especially glycerol surplus generated as a byproduct during the process of biodiesel. The surplus of glycerol will rise in the future since the notable increase of biodiesel process worldwide. Owing to the glycerol distribution and requirement market is stable and cannot be handled too much of glycerol produced from manufacturing

biodiesel properly, so the amounts of glycerol overflow in the market [13]. So, new application or new value-add product from glycerol has been making by a various of chemical reaction. In the past many years, there are so many transformation of glycerol have been studied for example etherification, oxidation, esterification, dehydration, acetylation, reforming, enzymatic, and hydrogenolysis [14]. As show in Figure. 2.3

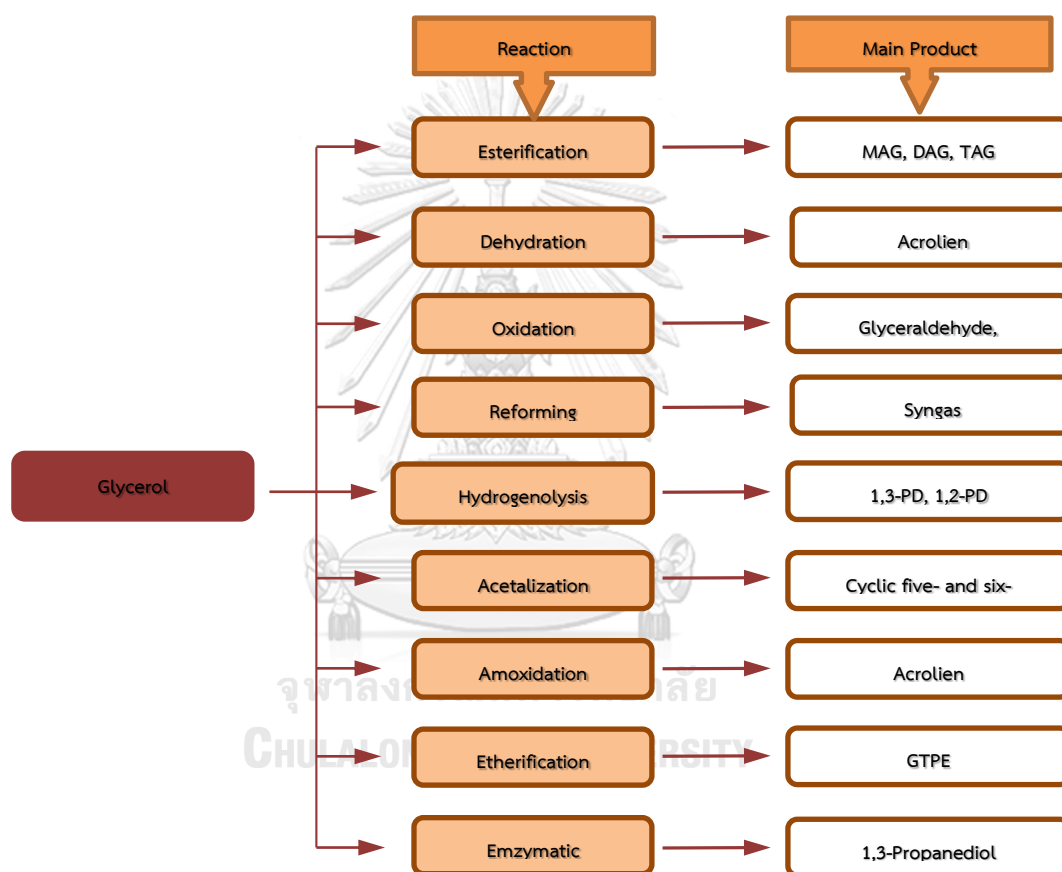


Figure 2.3 Routes for the glycerol conversion process

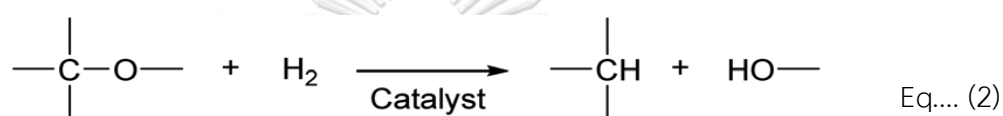
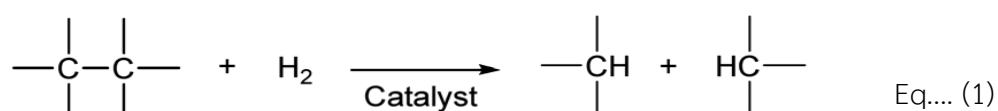
Among the entire product from conversion of glycerol, 1,3-propanediol is most famous material that can be used for vary application especially using to produce polymethylene terephthalate (PTT) and can be generated many industrial production likes coating, fiber, cosmetics, food, lubricant, medicine, adhesive or use as a solvent to produce an antifreeze. Since The worldwide of 1,3-propanediol

product is steadily increasing , having already raise almost 45,300 t per year. This growth is owing to the various applications in the manufacture of value-added products of 1,3-propanediol. Since, 1,3-propanediol is a significant intermediate chemical in the production of industrial for polyurethane and polyester. It is approximated that in year 2019, global trade for 1,3-propanediol will be rise up to 150,000 t per year, with approximates that the cost of 1,3-propanediol will gain from US \$157 million in 2012 to US \$560 million in 2019 [15, 16]. Another chemical product from glycerol mentioned was 1,2-propanediol. This is a value product that has the manufacturing of products. The amount of propanediol production was around 1 million tons per years in the United States [17]. 1,2-propaindiol can be generated without glycerol i.e. the hydration of ethylene oxide and propylene oxide. This product was imported in polyester resins [18].

The production of 1,3-propanediol is restricted and the prices are much more than 1,2-propanediol and the process for generating 1,3-propanediol are various for example hydroformylation of ethyleneoxide followed by hydrogenation, hydrate and hydrogenate of acrolein, and glycerol fermentation and glucose but all of the methods have problem with selective of 1,3-propanediol. Thus, the glycerol hydrogenolysis to 1,3-propanediol is an optional process that could be help to solve the problem if the catalytic efficiency has been developed [19].

2.2 Hydrogenolysis reaction of glycerol to 1,3-PD

The hydrogenolysis reaction is a sort of decrease reaction that connects with chemical separation in an organic compound of reactant for example carbon-carbon or carbon-oxygen by using hydrogen addition to disintegrate chemical molecule bonding.



The C-C or C-O single bond atom is cleaved or disintegrated by hydrogen in the reaction and the result is length of carbon atom has been decreased. Since glycerol has more hydroxyl bonds than propanediols. Hence hydrogenolysis of glycerol to propanediols involves the elimination one of -OH group and the increasing one of hydrogen species, similarly, the decrease of H₂O and the adding of H₂ molecules [20]. When the reaction proceed if the diminish of the primary -OH group of glycerol generates 1,2-propanediol, while disengagement of the secondary -OH group forms 1,3-propanediol. The challenging reactions in glycerol hydrogenolysis were generating by-product such as the cleaving of C-C bond to form ethylene glycol, the hydrogenolysis of glycerol in C-C or C-O bonds can be obtained more products like alcohols products such as methanol or ethanol or alkenes products (Figure. 2.4) [21].

In the past few decades, there are many researchers have been investigated the hydrogenolysis of glycerol mechanism in which could be classified into three types. First is dehydration-hydrogenation reaction. Second is dehydrogenation-dehydration-hydrogenation and the last one is direct hydrogenolysis of glycerol. Scheme 1 Show the pathways of glycerol to propanediol product by hydrogenolysis.

Usually, the mechanism of hydrogenolysis reaction is specific. The factor depends on the type of catalyst. For example, the distinct acid or basic catalysts can conduct to various mechanisms. The stability of intermediate in the process is another important factor affecting the reaction mechanism. These properties are important variables for the type and quantity of the resulting product [22, 23].

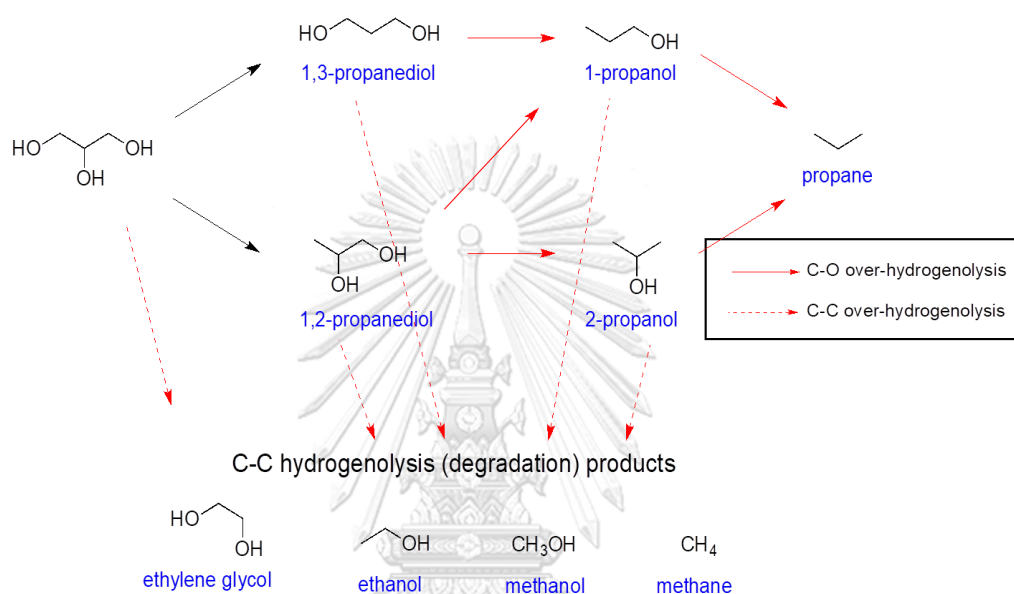
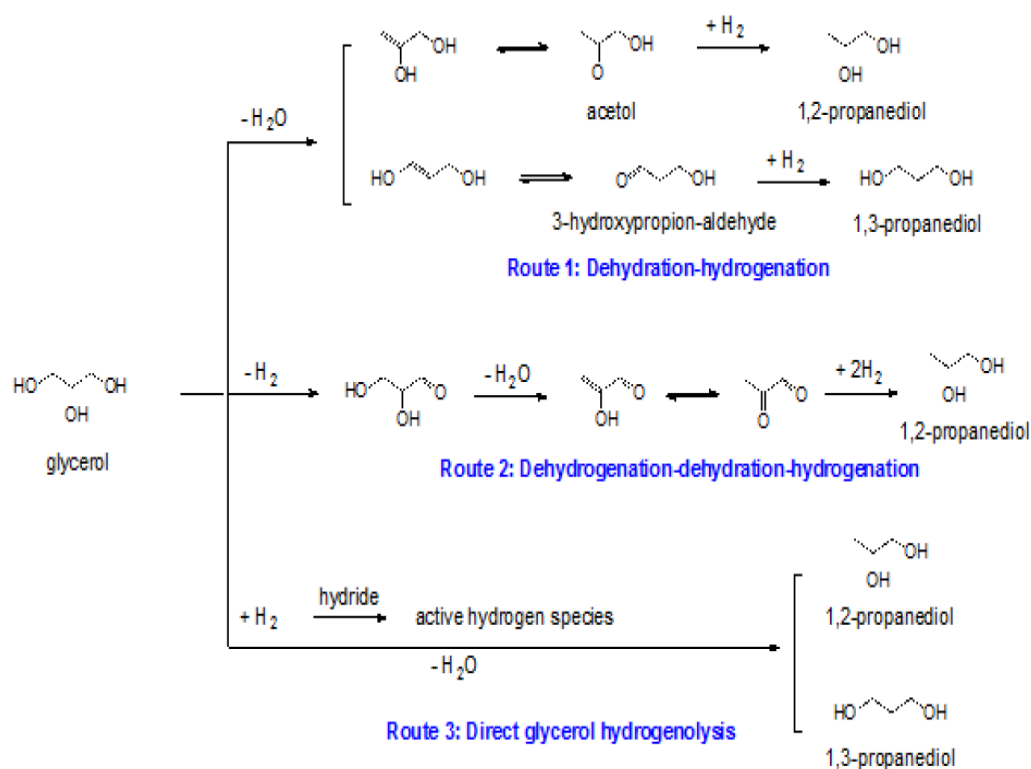


Figure 2.4 Byproduct from hydrogenolysis to 1,3-propanediol process [24].

2.3 Catalyst and Literature review



Scheme 2.1 The pathways of glycerol to propanediol by hydrogenolysis reaction [21]

Considering the catalysts have been used in the glycerol hydrogenolysis, it is found that, to selected catalyst for the hydrogenolysis reaction; it can be divided into two groups. First the acidity or basic of catalyst use for eliminates a hydroxyl group. Usually metal oxides supports are helped to provide acidic and basic. Second part is the reduction - oxidation of H_2 gas in the hydrolysis method. Basically, transition metals catalyst or noble metals have role in hydrogen stimulation. The first row of transition metals: Cu, Ni and Co has an ability to activate hydrogen molecules. Thus the entire of this metal have been applied in the reaction. Although transition metals have low price and have ability to withstand higher toxic by tracking impurities but the mainly product must be 1,2-propanediol [25]. Then noble metals are used to replace because it has capability to stimulate hydrogen molecule as well.

In 1989 and 1991 Montassier *et al.* reported the glycerol hydrogenolysis reaction to propanediol over Ru/C catalyst at 110-260 °C and 3-6 MPa. The mechanism is dehydrogenation-dehydration-hydrogenation (route 2, scheme 1). First, dehydrogenation reaction is carried out at the surface of the metal and glycerol is dehydrogenated to glyceroldehyde (intermediate). Next step, dehydration of glyceroldehyde was transformed to 2-hydroxyacrolein and pyruvaldehyde. Then two intermediate was converted to 1,2-propanediol with hydrogen addition in hydrogenation step and there are only few of 1,3-propanediol [26-28]. In addition, researchers found that basicity of reaction enhance rate of reaction for dehydration of glyceroldehyde similarly to the research of Lahr in 2003, 2005 [29, 30] and Maris in 2007 [31].

In 2005 Dasari *et al.* compared the catalytic on different catalysts in hydrogenolysis of glycerol at 180 °C and 1.4 MPa. Copper-chromite prepared by co-precipitation method has a good activity and high selectivity (85.0%) more than other metal (Pd/C, Pt/C and Ru/C). The pretreated of Cu component stimulates hydrogen species and chromium oxide supports are provided the acidic functionality to eliminate OH-groups (Figure 2.5) [32].

In 2007, Furikado *et al.* compared the activity over different noble-metal support over SiO₂, C and Al₂O₃ at 120 °C, 8 MPa. Rh/SiO₂ show a highest conversion (7.2%), including the selectivity of 1,3-propanediol and 1,2-propanediol (8% and 38 % respectively) because the reducibility of Rh species on support materials can greatly influence the performance of hydrogenolysis reaction of glycerol [33].

In 2012, Kim *et al.* were studied effect of Pd over CuCr₂O₄ (Pd_{0.5}-CuO/CuCr₂O₄) over the hydrogenolysis of glycerol to 1,2-propanediol. The result shows that Pd was discovered well dispersed on a surface of CuCr₂O₄ spinel structure. The highly dispersion of Pd enhance ability of Pd/Cr₂O₄ to utilized hydrogen, resulting in an

increase the activity of catalysts at low hydrogen pressure. The yield of 93.9 % with the selectivity reaching to 100% for 1,2-propanediol at 4 MPa. Furthermore, the synthesis of heterogeneous catalyst by co-precipitation method could be prepared with metals oxide such as ZnO, MgO, ZrO₂, Al₂O₃ etc [34-40].

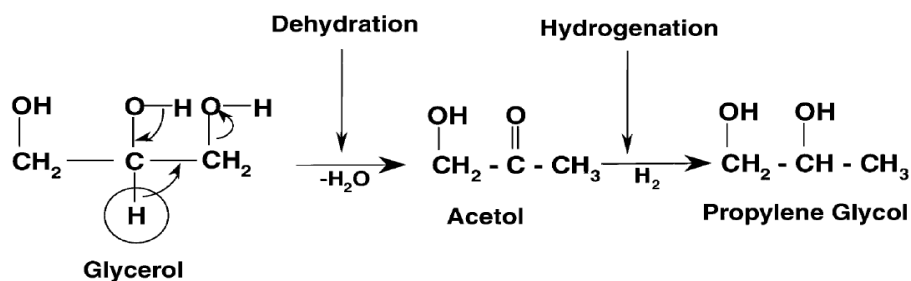


Figure 2.5 Proposed reaction mechanism for conversion of glycerol to propylene glycol [32]

In 2010-2012, Shinmi and Tomoshige reported, Using Rh-ReO_x/SiO₂ and Ir-ReO_x/SiO₂) as a catalysts for hydrogenolysis reaction of aqueous glycerol at 120 °C and 8 MPa. The result shows that a high of 1,3-propanediol selectivity. The mechanism is direct hydrogenolysis of glycerol. Glycerol absorbed over ReO_x surface at the primary or secondary of -OH group to form an intermediate, which is 2,3-dihydroxypropoxide and 1,3-dihydroxypropoxide, respectively. (Figure 2.6) Next, metallic Ir arouse proton to attack secondary position of 2,3-dihydroxypropoxide to produce intermediate 3-hydroxypropoxide. And then, the hydrolysis of 3-HPA generates 1,3-propanediol but if proton attack third position of 1,3-dihydroxypropoxide. The product would form to 1,2-propanediol. Although the reaction have to intermediate but 2,3-dihydroxy has a Hexagonal chemical compound that has a stability more than heptagonal chemical compound. Thus the reaction is selectively to form 1,3-propanediol. This mechanism also found in hydrogenolysis reaction over Rh-ReO_x/C reported by Chia el al [20, 22, 41-43].

In 2012, Tao *et al.* were synthesized mesoporous tungsten trioxide (m-WO₃) and commercial WO₃. The preparation of m-WO₃ catalysts were using an evaporation-induced self-assembly method and were supported by Pt precursor. all of the catalyst prepared by impregnation method and then impregnation of H₂PtCl₆ followed by calcination in air atmosphere at 400 °C and pretreatment in H₂ at 300 °C. Pt/WO₃ and Pt/m-WO₃ used in hydrogenolysis reaction of glycerol at 180 °C 5.5 MPa for 12 h. the major product is 1,3-propanediol. The Pt/WO₃ gained 4.5% of glycerol conversion and 29.9% of 1,3-propanediol selectivity. The comparison between m-WO₃ and commercial, illustrate that, the m-WO₃ show a good reducibility and high surface area of catalyst than commercial led to enhances dispersion of metal (Pt) over the surface support [44].

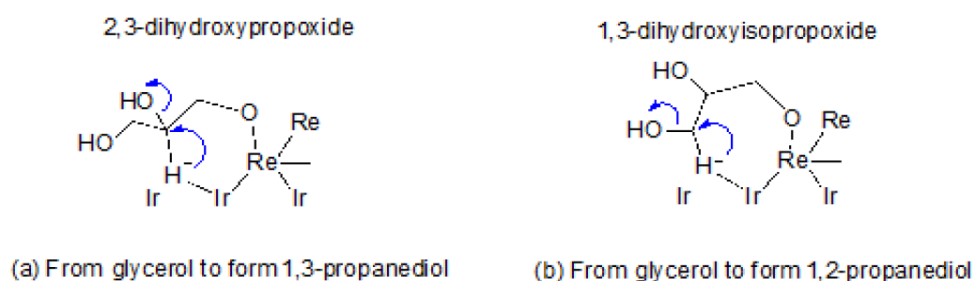
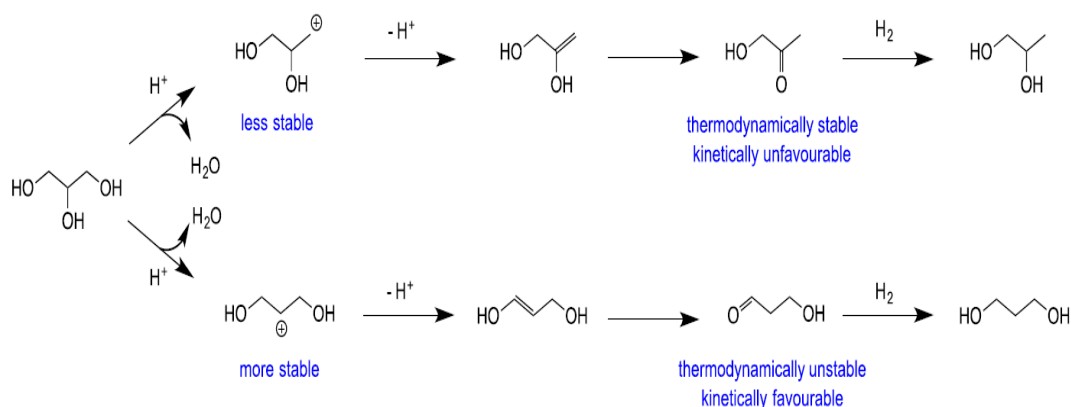


Figure 2.6 Model structures of the transition states of the hydride attack to the adsorbed substrate in the glycerol hydrogenolysis [22].

The selective for 1,3-propanediol from hydrogenolysis of glycerol reaction, at first procedure of mechanism, the glycerol dehydration to form carbocation intermediate. It should be noted that if the dehydration step formed primary carbocation intermediate instead of secondary carbocation intermediate, the main product should be 1,3-propanediol. The secondary carbocation was stable more than primary carbocation.

After that the protonation of two intermediate (secondary carbocation, primary carbocation) were transformed to 3-hydroxypropanol and acetol respectively, in final step both of two intermediate will generate to 1,3-propanediol and 1,2-propanediol respectively. (Scheme 2) 3-hydroxypropanal formation is kinetically like to acetol, even though thermodynamically unfavorable. Thus the quick hydrogenation of 3-hydroxypropanal very important before it transform to acetol. The increasing of 1,3-propanediol can be enhanced by increased of H₂ pressure might be due to boosted hydrogenation rate and stabilizing 3-hydroxypropanol. Based on this mechanism, it was found that Pt can dissociate hydrogen in to hydrogen species atom (proton (H⁺) and hydride (H⁻)) followed by spill over to WO₃ support (Brønsted acid sites). In addition to W⁵⁺ was generated from the reducibility of WO₃ can stabilize secondary carbocation to increase 1,3-propanediol product [20].

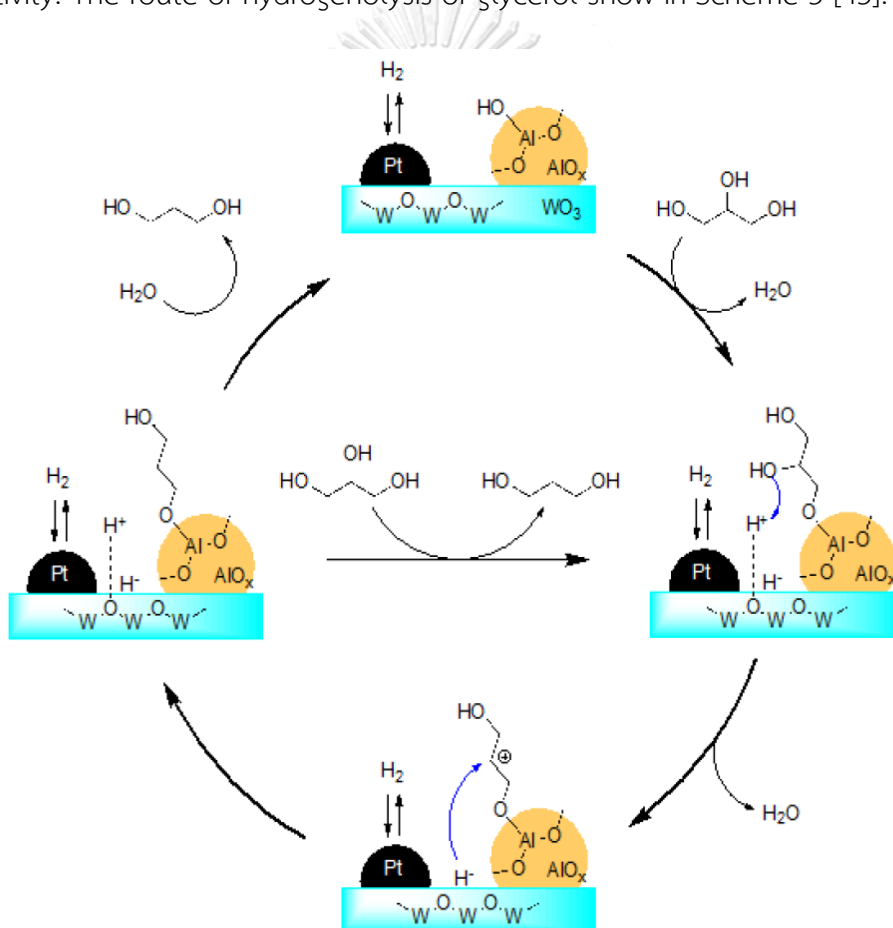


Scheme 2.2 Mechanism of hydrogenolysis of glycerol reaction with Pt/WO₃ catalyst [20].

After in the year, 2013 Kaneda et al. studied hydrogenolysis of glycerol to 1,3-propanediol over a Platinum/Tungsten Support on Boehmite Catalyst. The wet-impregnation method was used to prepare Pt/WO_x/AlOOH. The dispersion of WO_x over AlOOH can be achieved direct an ion-exchange process using ammonium (para)

tungsten and calcination at 800 °C and then H_2PtCl_6 solution mixed with WO_x/AlOOH stirred for 16 h and calcined at 300 °C.

It was found that after calcined at 800 °C. Boehmite was transform into $\gamma\text{-Al}_2\text{O}_3$. The reaction was carried on 180 °C, 5.0 MPa. The yield of 1,3-propandiol is 66%. Due to the Al-OH affects the glycerol absorption on surface support and stabilize the intermediate (3-hydroxypropanol) led to a high of 1,3-propanediol selectivity. The route of hydrogenolysis of glycerol show in Scheme 3 [45].



Scheme 2.3 The mechanism of glycerol hydrogenolysis to 1,3-propanediol over $\text{Pt-AlO}_x/\text{WO}_x$

In 2016, Sara et al. was purposed WO_x effect to the selective of glycerol hydrogenolysis to 1,3-propanediol over $\text{Pt}/\text{WO}_x/\text{Al}_2\text{O}_3$. The result show that WO_x has

an essential role in glycerol hydrogenolysis reaction: (1) WO_x express as a strong anchor site for the primary $-\text{OH}$ groups of glycerol, (2) WO_x provide H_2 species (protons), and (3) WO_x was stabilize the secondary carbocation. Catalytic test was carried on $200\text{ }^\circ\text{C}$, 9 MPa. The 1,3-propanediol yield approach to 38.8% [46].



CHAPTER III

EXPERIMENTAL

3.1 General

The chemical product such as 1,3-Propanediol (1,3-PDO) and 1,2-Propanediol (1,2-PDO) were acquired from Wako Pure Chemicals Co. The precursor chloroplatinic acid hydrate (H_2PtCl_6), Glycerol, and AMT (ammonium(meta)tungstate) was obtained from Sigma-Aldrich, Plural boehmite was purchased from Plural.

3.2 Catalyst Preparation

The Procedure of preparation of catalyst followed by the detail below

3.2.1 $\text{WO}_x/\gamma\text{-Al}_2\text{O}_3$

First, AMT (8%wt) was dissolved in DI water stirred at 25 °C and maintaining this temperature until it completely dissolved. Then AlOOH 10 g was mixed to the aqueous solution, stirred at ambient temperature for 16 h. The solution and catalysts was filtrated and dryness at 110 °C for 12 h. Then the solid catalyst smashed into powder. Then calcination temperature of catalyst was at 800 °C and 900 °C for 3 hr. air atmosphere.

3.2.2 $x\%\text{Pt}/\text{WO}_x/\gamma\text{-Al}_2\text{O}_3$

The Chloroplatinic acid hydrate dissolved in 50 mL DI water and 2 g of support was mixed to this solution, following by stirring for 16 h at room temperature and then evaporation 12 h at 110 °C. The solid catalyst was smashed into powder and then calcination at 300 °C for 3 h under an air atmosphere to get $\text{Pt}/\text{WO}_x/\gamma\text{-Al}_2\text{O}_3$. These catalyst are denoted as $x\text{Pt}/y\text{WO}_x/\gamma\text{-Al}_2\text{O}_3$, where x related to the platinum loading in weight percent (wt %) in the complete catalysts and y refer to the WO_x loading associated with the gamma-alumina support.

3.2.3 x%Pt/WO_x/Al₂O₃ reduced catalyst

H₂PtCl₆ dissolved in 50 mL DI water and then added 2 g of WO_x/AlOOH, following by stirring 16 h at ambient temperature. Then catalyst evaporated at 110 °C 12 h. The solid catalyst was smashed to powder. Catalyst was calcined at 300 °C under an air for 3 h. After that, the catalysts were further pretreated under H₂ atmosphere at 300 °C for 1 h.

3.3 Typical Hydrogenolysis Reaction

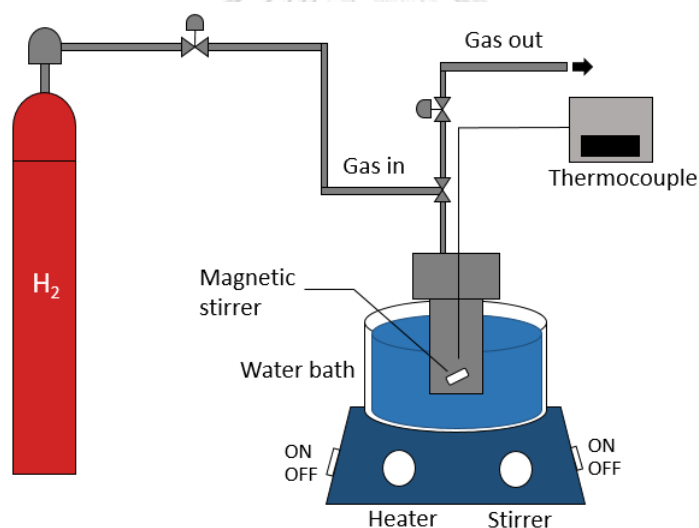
The reaction was carried out in a autoclave (100 mL) equipped with Teflon vessel. Usually, 10 mmol of glycerol was placed to DI water (30 mL) and 1.5 g of catalysts was settled in Teflon vessel (Figure 3.1). Stirring at 800 rpm, purged with H₂ gas 3 times at 5 bar (10 min/times), and then heating up to 140 °C, 5 bar for 12 h. After finish, the reactor was cooling in an ice-water bath for 3 h, and then the gas in reactor was discharged. The aqueous product was analyzed by GC (Shimadzu GC-14B, Japan) equipped with a flame ionization detector (FID), using a DB-WAX capillary column (30m x 0.32mm x 0.25um). The details and conditions of gas chromatography are presented in Table 3.1.

$$\text{Conversion \%} = \frac{\text{Moles of glycerol (in)} - \text{Moles of glycerol (out)}}{\text{Moles of glycerol (in)}} \times 100$$

$$\text{Selectivity \%} = \frac{\text{Moles of one product}}{\text{Moles of glycerol (in)} - \text{Moles of glycerol (out)}} \times 100$$

Table 3.1 The analysis conditions for GC-FID

Gas chromatography	Shimadzu GC -2014
Detector	FID
Column	DB-WAX capillary column
Carrier Gas	Helium (99.99 vol. %)
Make-up Gas	Air (99.9 vol. %)
Column Temperature	100°C
Injector Temperature	230°C
Detector Temperature	250°C
Time Analysis	20 min

**Figure 3.1** Experimental equipment for hydrogenolysis of glycerol reaction

3.4 Catalyst Characterization

To understanding structure, texture properties and mechanism of catalyst, the characterization technique were used by various technique followed as detail below.

3.4.1 X-ray diffraction (XRD)

To determined patterns of catalysts (XRD), the catalysts were characterized by Bruker D8 Advance using Cu K α irradiation at range 20° to 80° with a step of 0.05° s⁻¹.

3.4.2 X-ray photoelectron spectroscopy (XPS)

To investigate the surface composition and binding energy, X-ray photoelectron spectroscopy was analyzed on using an Amicus photoelectron spectrometer with Mg K α X-ray source at current of 20 mA and 10eKV. To obtain binding energy, the binding energy value was measured by the C 1s peak at 284.6 eV.

3.4.3 CO-Pulse Chemisorption

The active sites of platinum metal were investigated by CO pulse chemisorption technique using Micromeritics ChemiSorb 2750 and ASAP 2101C V.3.00 software. 50mg of catalysts pretreated in H₂ at 185 °C for 1h. After reduction, H₂ was driven by He gas at 195 °C for 30 min. Then cooling sample to ambient temperature with Helium gas. After cooling down, the 20 μ l of CO gas was driven to the catalyst by syringe injection at a flow rate of He is 25 ml/min at 30 °C. CO was injected until catalysts were saturated. The Pt active sites catalysts were evaluated by presuming that ratio of CO adsorbed/Pt atom is identity.

3.4.4 N₂-physisorption

N₂ adsorption–desorption experiments were observed to the catalysts at -196 °C by under vacuum 12 h the multipoint Brunauer–Emmett–Teller (BET) method on a Micromeritics ASAP 2020 equipment. First the analysis, the sample was pretreated under vacuum at 300 °C for 8 h.

3.4.5 Scanning electron microscope (SEM)

The chemical composition attributed on a surface of the catalysts was examined with SEM-EDX using Link Isis series 300 program SEM (JEOL model JSM-5800LV).

3.4.6 X-ray absorption spectroscopy (XAS)

XAS characterize are performed at synchrotron sources that transfer intense (10¹⁰ photons per s or better) X-ray beams to the catalyst. In EXAFS examination, the data of the electrical properties and environmental structure of the X-ray-absorbing atom and its background is removed from the X-ray absorption coefficient $\mu(E)$ calculated in range 1000–1500 eV from the X-ray absorption edge energy. EXAFS spectra were investigated using REX2000 software (Ver. 2.5, Rigaku) [47-49]. The energy was referred using the inflection point of Pt foil, K₂PtCl₄, PtO₂ and WO₃, which was fixed to be 11563 eV.

3.4.7 NH₃-TPD

NH₃-TPD Technique was performed using Chemisorb 2750 (Micromeritics) with different procedures as follows; the acidity and basicity of the samples were tested by NH₃. Catalyst powder 0.05 g pretreated with He gas at 510 °C for 1h, and then cooling down to 30 °C. After that, 25 ml/min of 15% NH₃/He was added through sample for 30. Then, the catalysts were purged with He gas until the baseline was stable. The desorption profile (30°C - 500°C) was recorded by a TCD. The heating rate is 10°C/min.

3.4.8 IR spectra of pyridine adsorption

To determine the types of acid sites of the catalysts, the FT-IR of adsorbed pyridine was analyzed with a Bruker Equinox 55 FT-IR spectrometer having mercury cadmium telluride (MTCB) detector. The 0.04-0.05 g of sample was preheated at

300°C for 1 hr. with 10°C/min in a vacuum. After that the operating temperature was cooled to 50°C to absorb the pyridine for 10 min. the sample was evacuated for 40 h at 50°C and the IR spectra was collected at 50°C. The intensity of the Brønsted and Lewis acid sites in each sample was calculated from the subtraction of the IR spectra after sample pretreatment from IR spectra of sample evacuation at 50°C for 1 h.

3.4.9 IR spectra of ammonia adsorption

NH₃-IR spectra were collected with Bruker Vertex-70 FT-IR spectrometer equipped with a Harrick Praying Mantis attachment for diffuse reflectance spectroscopy. About 0.03–0.05 g of catalyst was settled in a Harrick cell. The catalyst was pretreated at 500°C (heating rate = 10°C/min) with N₂ gas. Maintaining the temperature for 1 h under H₂/N₂ gas, then the catalysts was heating to 550°C with the similar heating rate under N₂ gas. The sample was cooled to 40°C. After that the 15% NH₃/He mixed gas was added to the catalyst until sample was saturated with for 30 min. The NH₃/He was desorbed with nitrogen gas stream about 40 min. The spectra were recorded using a MCT detector.

3.4.10 Temperature-programmed desorption of hydrogen (H₂-TPD)

The sample of H₂-TPD was examined with the Micrometrics Chemisorbs 2750 automatic system with a thermal conductivity detector. The non-pretreated and pretreated catalysts were introduced. The pretreatment of 0.05 g catalyst at 550°C under pure H₂ flow (flow rate = 25 ml/min) for 1 h, after 1 h the sample was heated to 550°C for 30 min under N₂ flow. Finally, cooling sample down to 40°C with N₂ flow. The saturation of pure H₂ was added to sample about 30 min and the H₂ gas was changed to N₂ and finally a TPD test was performed at 800°C with the heating rate 10°C/min.

3.4.11 Temperature-programmed reduction of hydrogen (H₂-TPR)

To determine the reducibility of the sample catalysts, H₂-TPR profiles were investigated by using the Micrometrics Chemisorbs 2750 automatic system with a thermal conductivity detector. First, 0.05 g of sample was pretreated in Ar. The flow rate is 25 ml/min at 350°C for 1 h. Then cooling the catalyst to 40 °C, the streaming of gas changed to 10% H₂ mixed in Ar. The flow rate is 15 ml/min. Finally, the catalysts were heated up and started at 40°C to 800°C with a temperature rate of 10°C/min.



CHAPTER IV

RESULTS AND DISCUSSION

This chapter contains of several studies involving the effect of calcination on support to catalytic activity, the H₂ influence to catalytic activity, %loading of Pt and tungsten oxide to catalytic activity and effect of reduction process on catalytic activity which affects performance of hydrogenolysis of glycerol reaction. The characterizations of samples were investigated by N₂-physisorption, SEM-EDX, XRD, XPS, XAS, NH₃-TPD, NH₃-IR, Py-IR, H₂-TPD, H₂-TPD, and CO pulse chemisorption technique.

4.1 Effect of calcination temperature to catalytic activity

The diffraction line of XRD of 2%Pt/WO_x/γ-Al₂O₃ catalysts over different calcination temperature of support is displayed in Figure 4.1.

4.1.1 X-ray diffraction (XRD)

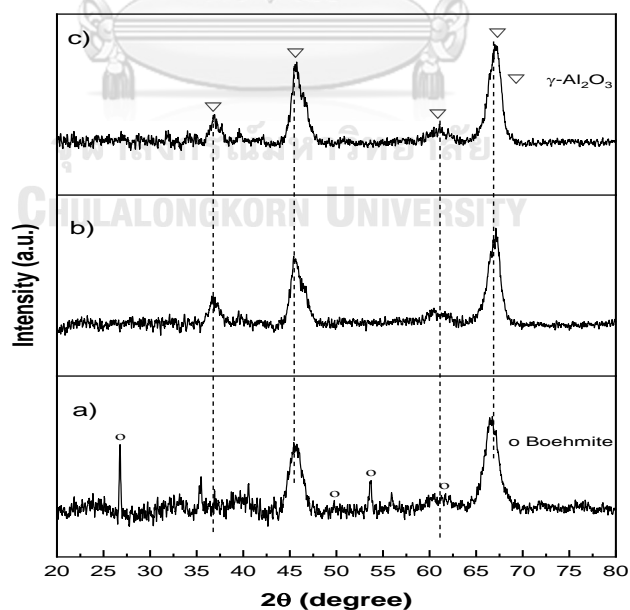


Figure 4.1 XRD patterns of a) 2%Pt/WO_x/boehmite (800 °C)

b) 2%Pt/WO_x/γ-Al₂O₃ (900 °C) and c) WO_x/γ-Al₂O₃

As seen in Figure 4.1, all of two catalysts showed the diffraction lines at 37.4, 46.0 50.3, 60.35 and 67.0° and were corresponding to support γ -Al₂O₃ [50]. The 2%Pt/WO_x/AlOOH catalysts calcined at 800°C appeared diffraction peaks at 14.2, 27.1, 49.6 and 64.8° that correspond to boehmite [51]. It found that at 800 °C calcination temperature, the boehmite phase mostly transformed to γ -Al₂O₃ but it still seen some of boehmite phase on surface catalyst due to the interaction strongly between WO_x species with sites over the γ -Al₂O₃ surface. These surface species inhibit the sintering of boehmite and the structural transformation of boehmite into γ -Al₂O₃ during high temperature oxidation treatments [52]. The 2%Pt/WO_x/AlOOH and 2%Pt/WO_x/ γ -Al₂O₃ catalysts were not observed peak of platinum oxide or platinum metallic. It may be due to the co-operation of WO_x and γ -Al₂O₃ for dispersing Pt well over supported catalyst [53]. The X-ray diffraction (XRD) lines of the catalyst did not express the species peaks of WO_x, indicating that the constant dispersion of WO_x species on the support surface, in well agreement with SEM-EDX result (Figure 4.2). From XRD result, the preparation of WO_x/AlOOH by wet impregnation procedure and then calcination temperature at 800 °C. it was found boehmite almost entirely formed to γ -Al₂O₃ phase. After the enhancing of the temperature calcined from 800°C to 900°C, the phase of boehmite completely change to γ -Al₂O₃. Thus, the comparison of catalytic activity between 2%Pt/WO_x/boehmite and 2%Pt/WO_x/ γ -Al₂O₃ was studied.

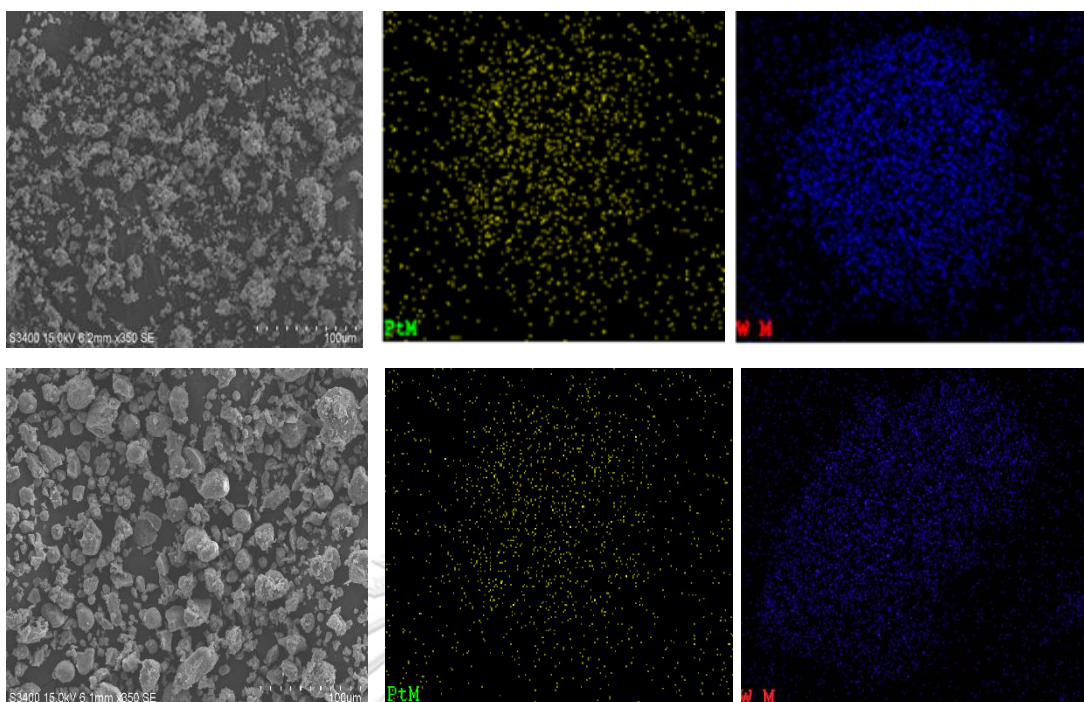


Figure 4.2 SEM images of catalysts (top) 2%Pt/WO_x/γ-Al₂O₃ (bottom) 2%Pt/WO_x/AlOOH

4.1.2 N₂-physisorption

The physical properties catalyst is express in Table 4.1. The surface area of the catalysts sample was decrease with all of the catalysts by compared with the support (SABET of AlOOH = 180 m² g⁻¹, SABET of WO_x/γ-Al₂O₃ = 89 m² g⁻¹ and SABET of WO_x/AlOOH = 82 m² g⁻¹) as the WO_x loading increase. This may be due to the hindering or adding of supported pores during the tungsten oxide was conducted. The interaction of the tungstate supported platinum oxide had the similarly affected and can be described through the same assumption [25, 45]. The constant CO uptake was explanations the dispersion of Pt equal to 25.2% for 2%Pt/WO_x/γ-Al₂O₃ catalyst which much more than 2%Pt/WO_x/AlOOH (24.4%).

Table 4.1 N₂-Physisorption, CO-Chemisorption, acidities catalytic activities results of the impregnated catalysts.

Catalyst	CO Absorbed (μmol CO/g cat)	Pt dispersion (%)	Surface area (m ² g ⁻¹)	Total Acidity (mmol NH ₃ /g cat.)	Conversion of glycerol (%)*	Selectivity	
						1,3-propanediol	1,2-propanediol
WO _x /AlOOH (800 °C)	n.a.	n.a.	89	n.a.	n.a.	n.a.	n.a.
WO _x /γ-Al ₂ O ₃ (900 °C)	n.a.	n.a.	85	n.a.	n.a.	n.a.	n.a.
2%Pt/WO _x /AlOOH	40.8	20.4	73	1.15	32.8	18.2	5.6
2%Pt/WO _x /γ-Al ₂ O ₃	50.4	25.2	79	1.51	34.6	21.6	4.1

n.a.=non analysis

4.1.3 IR spectra of ammonia adsorption

The IR spectra determined after NH₃ adsorption illustrate in Figure 4.3. From the literature review [54], the acid sites are naturally decided and examined in range of the 1100–1800 cm⁻¹. The Brønsted and Lewis acid site of catalysts are accompanied to the product selectivity on hydrogenolysis of glycerol, which was normally examined by the NH₃-IR. The band at 1448, 1454, and 1460 cm⁻¹ were referred to the symmetric and asymmetric deformation form of the protonated NH₃ (NH₄⁺) correlated to Brønsted acid sites. The peaks at 1258, 1260, and 1293 cm⁻¹ were correlated to the symmetric and asymmetric disfigurement form of NH₃ correlated to Lewis acid sites. The Brønsted acid sites centered at 1448-1450 and Lewis acid sites were at 1258-1293 cm⁻¹, individually. According to Table 4.2, the phase of plural-boehmite formed to γ-Al₂O₃ was improved Brønsted and Lewis acidity. Suggesting

that Brønsted acid sites were derived from hydroxyl groups of surface catalysts binned on the discovered or well-dispersed tungstate of $\text{WO}_x/\gamma\text{-Al}_2\text{O}_3$, which it better than WO_x/AlOOH . The calculation of the Brønsted acids and Lewis acids sites demonstrated in Table 4.2 The band at 975 cm^{-1} is associate to the OH-groups of alumina [55].

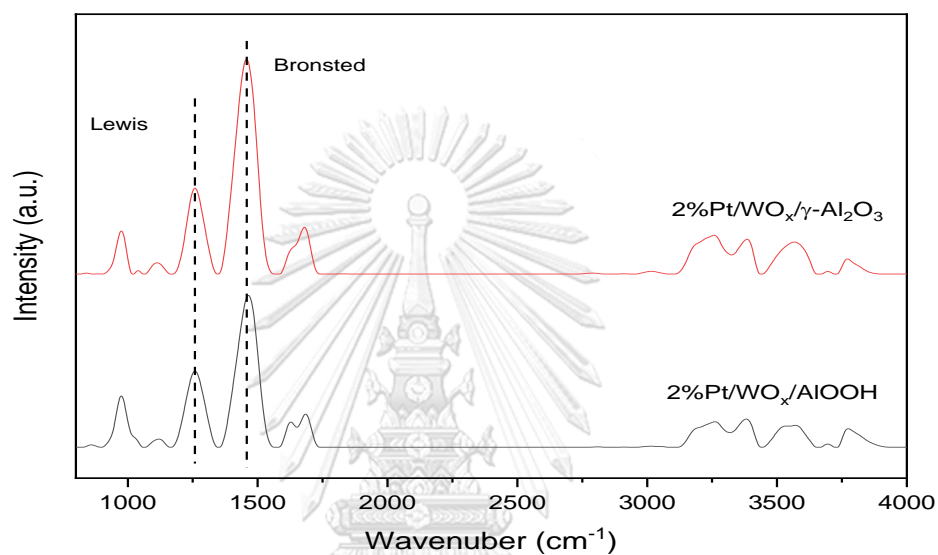


Figure 4.3 FTIR of adsorbed NH_3 on fresh $2\% \text{Pt}/\text{WO}_x/\text{AlOOH}$ (calcined at 800°C) and fresh $2\% \text{Pt}/\text{WO}_x/\gamma\text{-Al}_2\text{O}_3$ (calcined at 900°C) catalysts.

Table 4.2 The amounts of Brønsted and Lewis acid sites over the surface catalysts investigated with the in situ DRIFTS of adsorbed NH_3

Catalyst	Lewis acid (a.u.) ^a	Brønsted acid (a.u.) ^a	B/L acidity
$2\% \text{Pt}/\text{WO}_x/\text{AlOOH}$	1.3	11.9	9.1
$2\% \text{Pt}/\text{WO}_x/\gamma\text{-Al}_2\text{O}_3$	4.4	14.6	3.3

^a The amount of acid sites were calculated from the quantity of the desorbed ammonium from $\text{NH}_3\text{-IR}$.

4.1.4 NH₃-Temperature Programed Desorption

Figure 4.4 shows the calcination temperature affect to boehmite support (8 wt% WO_x content) on the activity of 2 wt%Pt/WO_x/γ-Al₂O₃ catalyst over hydrogenolysis of glycerol at 140 °C in 5 bar H₂ pressure. The information show certainly that the improving the calcination temperature of support introduced to an increasing the acid sites concentration on surface catalyst, i.e. acidity (a.u.) of support with various calcined temperatures, was determined by TPD of NH₃. it is showed in Table 4.1 Increasing the supported calcination temperature induced an enhance in the total acid sites surface from 1.15 NH₃/g catalyst on a 2%Pt/WO_x/AlOOH (800 °C) sample to 1.51 NH₃/g catalyst on a 2%Pt/WO_x/γ-Al₂O₃ (900 °C). According to Qin *et al.* research has studied the developing the supported calcination temperature is approving because it raise the concentration of H₂ species (H⁺, H) on Pt/WO₃/ZrO₂ [56].

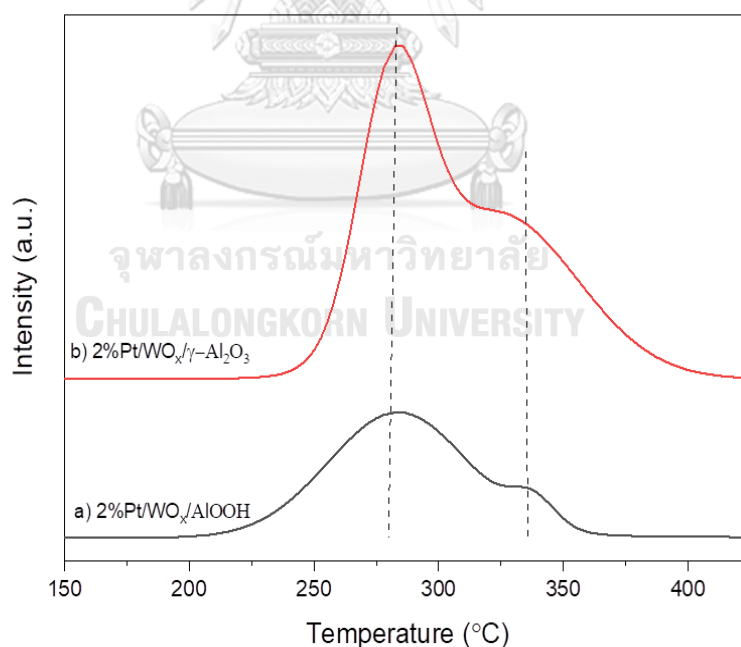


Figure 4.4 NH₃-TPD profiles of a) 2%Pt/WO_x/AlOOH and b) 2%Pt/WO_x/γ-Al₂O₃ catalysts.

Figure 4.5 presents the data of the hydrogenolysis of glycerol with distinct supported catalysts. It was indicated that Pt/WO_x/γ-Al₂O₃ catalyst provided a notable glycerol conversion (34.6%) and 1,3-propanediol selectivity (21.6%). According to the result of NH₃-IR, Pt/WO_x/γ-Al₂O₃ displayed the high value of Brønsted acid site, which persuaded the development of 1,3-propanediol selectivity. However, the conversion of the distinct calcination temperatures influenced the glycerol conversion and 1,3-propanediol selectivity because the improvement of total acidity accompanied with Brønsted acid sites after calcination support at 900 °C. Brønsted acid sites have a significant role in glycerol dehydration to 3-HPA. The intermediate (3-HPA) hydrogenated over the surface of the catalyst produces 1,3-propanediol [57].

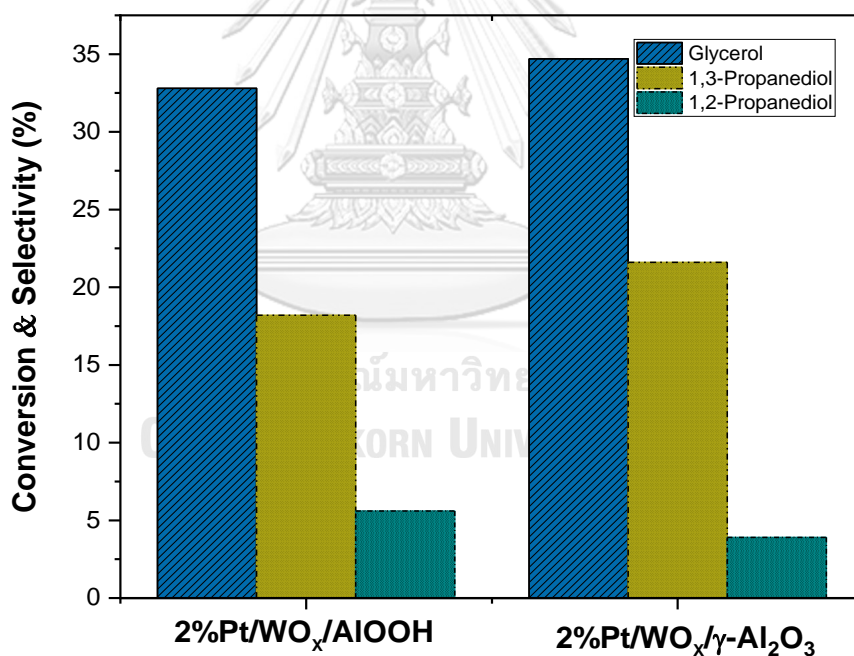


Figure 4.5 Glycerol conversion and product selectivity obtained from hydrogenolysis of glycerol over different catalysts.

4.2 Effect of Hydrogen pressure to 2%Pt/WO_x/γ-Al₂O₃

As seen in Figure 4.6, the influence of the H₂ pressure was considered in the range from 0 to 10 bars at reaction temperature 140 °C, 12 hr. and a stirring rate of 800 rpm. it can be found that the H₂ pressure increased from 0 to 10 bar, the glycerol conversion was gradually raise up from 14.7% to 43.7%. The increasing of the glycerol conversion was related to a slight enhance of the selectivity through 1,3-propanediol in range of 0-5 bar, further improving of H₂ pressure, the selectivity decreases to abruptly to 10.9 %. The highest selectivity of 1,3-propanediol (21.6%) was obtained at 5 bar. For 1,2-propanediol, its selectivity was no significant changed in the H₂ pressure improve from 0 to 10 bar. The remarkable effect of the hydrogen feed was on the glycerol conversion and propanediol selectivity with the suitable of H₂ pressure. The high glycerol conversion and selectivity of 1,3-propanediol were 34.6% and 21.6% ,respectively. In conclusion, the improvement of 1,3-propanediol due to the rate of hydrogenation enhanced in range 0-5 bar. The researcher can conclude the properly H₂ pressure is favourable to gain 1,3-propanediol in the glycerol hydrogenolysis, which seem to describe in the literature review [25, 53, 58, 59].

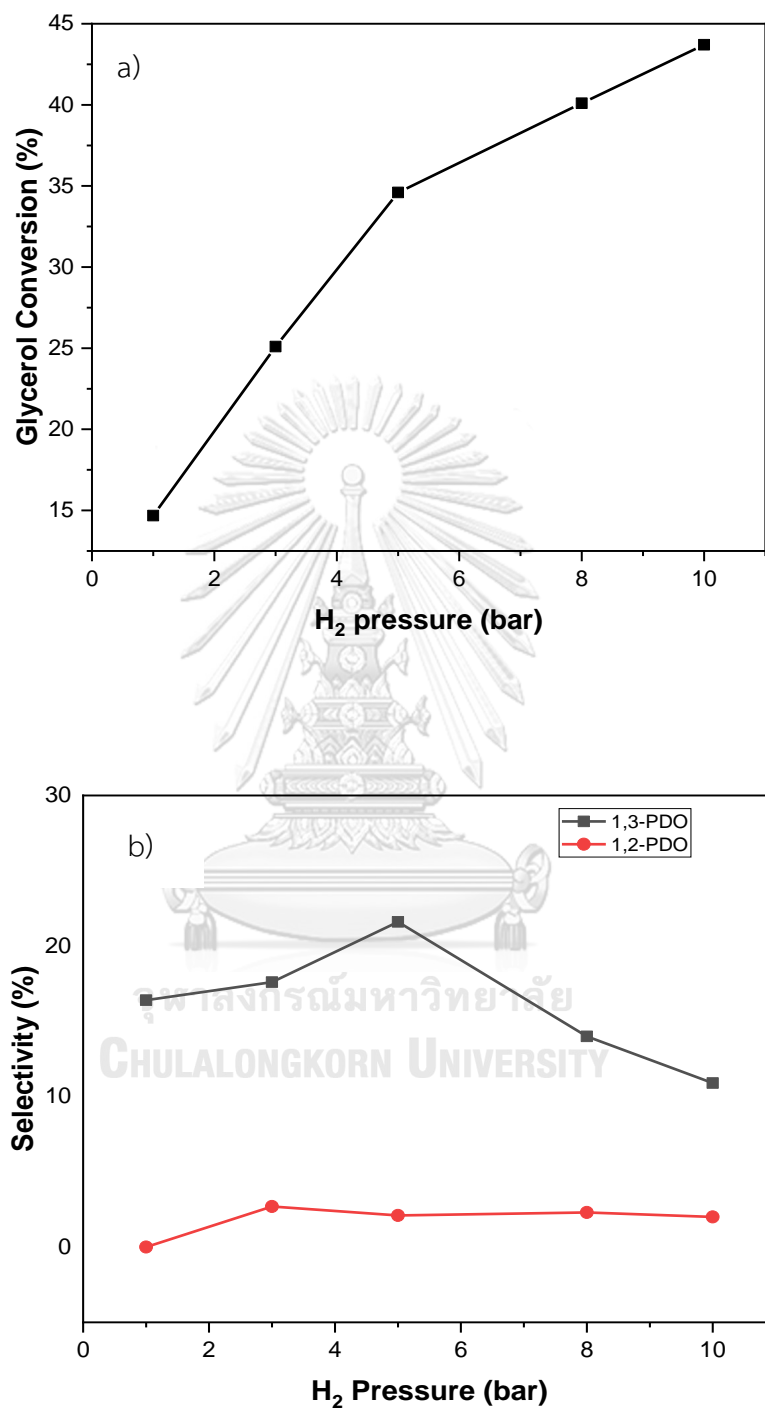


Figure 4.6 Effect of H₂ pressure on glycerol hydrogenolysis over 2%Pt/WO_x/γ-Al₂O₃ catalyst a) glycerol conversion and b) product selectivity

4.3 Effect of %Pt loading to catalytic activity

4.3.1 CO chemisorption

The existing of tungsten oxide in the Pt/WO_x/γ-Al₂O₃ do not absorb CO [60] so, CO chemisorption was analyzed the platinum metal dispersion and particle size on samples. The most general stoichiometry between CO adsorption/Pt metal for the estimation of the dispersion of Pt metal, that the ratio is 1:1. As shown in Table 4.3, the result demonstrate that the decline in Pt dispersion from 25.2% to 18.39% when the the Pt loading content increase from 2% to 8% and the CO uptake value also raise with the enhancing in Pt metal on the surface of WO_x/γ-Al₂O₃ support. This is probably due to growth up of Pt particle at higher loading. It can be concluded that when the amount of Pt increases to a proper content, the selectivity of 1,3-propanediol will be higher but when adding the amount of Pt more than the appropriate value, that the selectivity 1,3-propanediol decreased, while the conversion of glycerol increased indicated that Pt content excess.

Table 4.3 Physicochemical properties, acidities of Pt/WO_x/γ-Al₂O₃ with different %Pt loading content and activity result obtained after 12 h, 140 °C, and 0.5 MPa pressure.

Catalyst	CO absorbed (μmol CO/g cat)	Pt dispersion (%)	Total Acidity (mmol NH ₃ /g cat.)	Conversion of glycerol (%)	Selectivity (%)		
					1,3- PDO	1,2- PDO	ET and 1-PO
2%Pt/WO _x /γ-Al ₂ O ₃	50.4	25.2	1.58	34.7	21.3	2.0	44.8
5%Pt/WO _x /γ-Al ₂ O ₃	103.8	20.75	2.01	44.1	32.5	2.9	50.3
8%Pt/WO _x /γ-Al ₂ O ₃	147.2	18.39	2.58	60.16	16.9	1.2	41.7

PDO=Propanediol, PO= propanol

4.3.2 X-ray diffraction (XRD)

Figure 4.7 express the diffraction pattern of catalysts. All the catalysts illustrate characteristic peaks of γ -alumina. The XRD diffraction line of the catalysts with a maintain WO_x content (≈ 8 wt.%) and different Pt loading reveal that only diffraction peaks coresponded to γ -alumina cluster (at $2\theta = 37.5^\circ, 45.4^\circ, 50.3^\circ, 60.35^\circ$ and 66.9°) [61]. No diffraction lines of the WO_x groups were observed for all catalyst, indicating the forming of disperses tungstate species. There were no noticeable diffraction peaks of metal or oxide of the Pt, illustrating the pt metal has a good dispersion on all of the surface support.

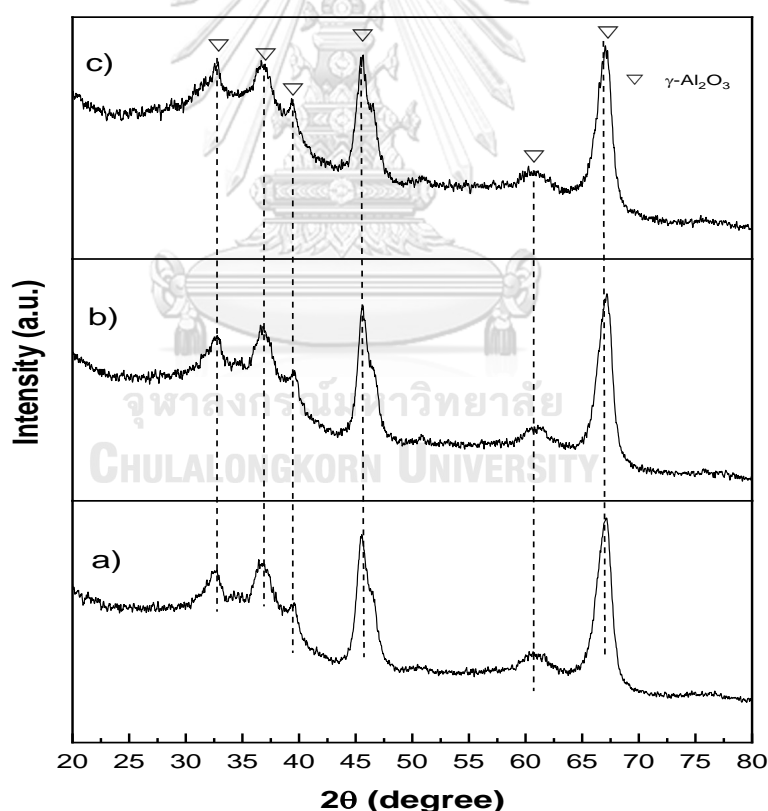


Figure 4.7 XRD patterns of the a) 2%Pt/ WO_x / γ - Al_2O_3 , b) 5%Pt/ WO_x / γ - Al_2O_3 , and c) 8%Pt/ WO_x / γ - Al_2O_3 catalysts.

4.3.3 NH₃-Temperature Programed Desorption

The NH₃-TPD profiles of distinct contents of Pt/WO_x/γ-Al₂O₃ catalysts are expressed in Figure 4.7. The number of acid sites (Table 4.3) can be determined from the area of desorption peak, and acid strength was estimated from the highest TPD peak. Normally, the maximum peaks of NH₃ can be indicated at three temperature areas to describe the class of acidic sites. First, the weak acid sites in temperature range at 150–300 °C. the second is the moderate acid sites at 300–450 °C, and the last one is strong acid sites at 450–650 °C [59]. The three catalysts expressed broad TPD profiles, indicating that the wide of acid strength on surface was distributed.

The NH₃-TPD result of Pt/WO_x/γ-Al₂O₃ catalysts displayed clear agreed noticed two desorption peaks in temperature ranges, that is low temperature region (285 °C) and medium temperature region (330 °C), which were corresponded to weak acid sites and moderate acid sites from the prior region is correlated to weak acidic sites, the second region distributed to desorption of NH₃ from medium acidic sites, respectively [50]. According to the results of NH₃-TPD from Table 4.3, the peak position displayed varies notably with a sharply narrow significantly after Pt impregnation; moreover, the total amounts of NH₃ adsorbed over the catalyst surge up with an addition in metallic Pt content. The quantitative evaluation of acid strength attribution in various regions of the amount of NH₃ desorbed was express in Table 4.3. The number of acidic sites was seen to improve with platinum from 2% loading up to 8 wt %, due to the addition of residual chlorine species in the catalyst as the H₂PtCl₆ was used as the precursor. As illustrated in Table 4.3. It also noticed with the development in the platinum content.

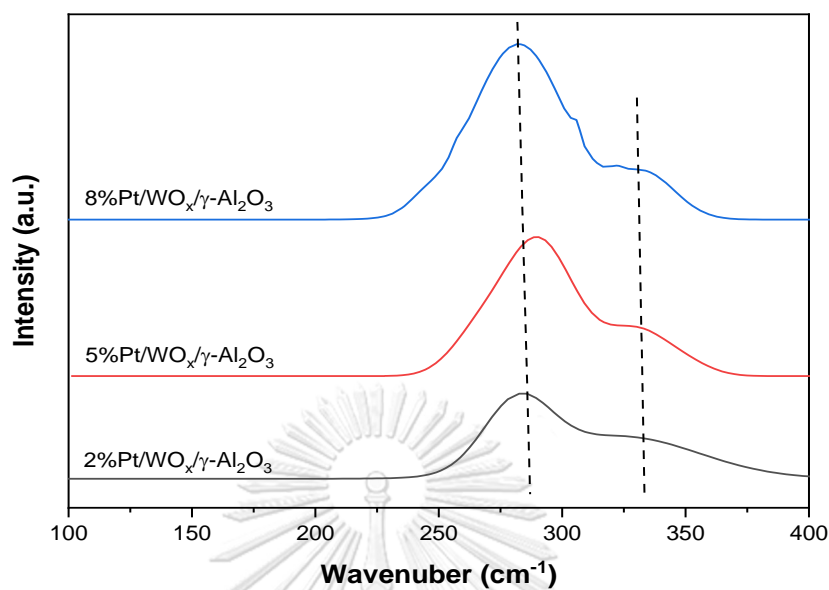


Figure 4.8 TPD of ammonia profiles of various %Pt loading supported on $\text{WO}_x/\gamma\text{-Al}_2\text{O}_3$ catalysts.

4.3.4 IR spectra of ammonia adsorption

The natural acid site of the catalysts was related to the product selectivity over hydrogenolysis of glycerol reaction, which was usually determined by the NH_3 -IR process. Figure 4.9 shows the NH_3 -IR spectra adsorbed on 2% 5% and 8% Pt on $\text{WO}_x/\gamma\text{-Al}_2\text{O}_3$ support catalysts in the region of $1400\text{-}1800\text{ cm}^{-1}$, the Brønsted acid sites were centered at 1480 and 1680 cm^{-1} . The band at ca. 1280 and 1620 cm^{-1} were related to Lewis acid sites [54], and the concentration of the Brønsted acids and Lewis acids sites listed in Table 4.4 was decided the area of adsorption bands integrate from 1480 cm^{-1} to 1280 cm^{-1} , respectively.

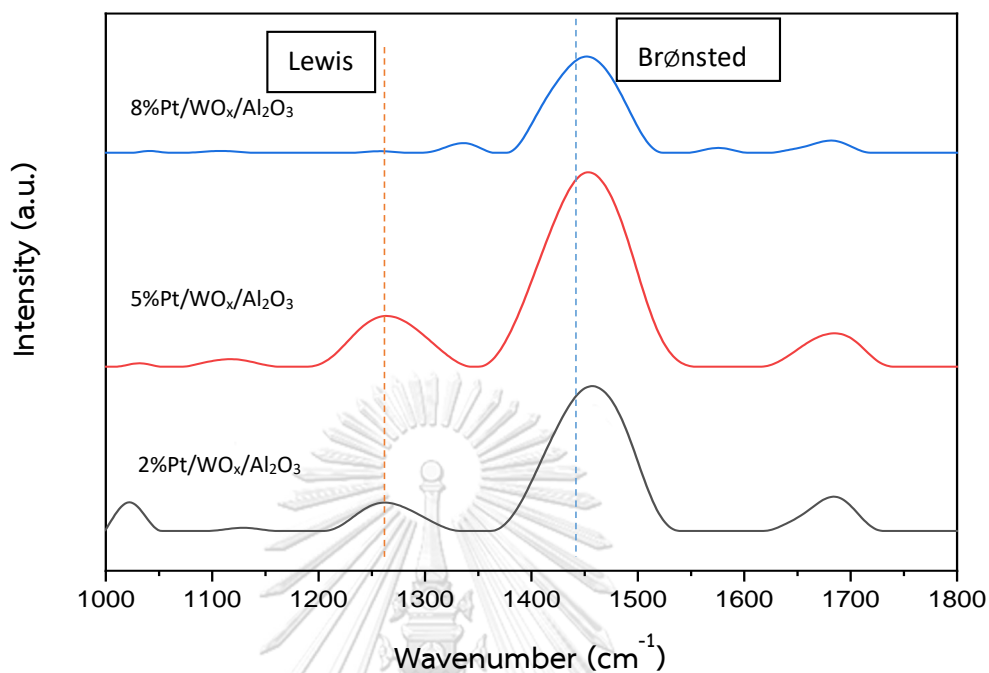


Figure 4.9 FTIR of adsorbed NH_3 on fresh 2%Pt/ $\text{WO}_x/\text{Al}_2\text{O}_3$, 5%Pt/ $\text{WO}_x/\gamma\text{-Al}_2\text{O}_3$ and 8%Pt/ $\text{WO}_x/\gamma\text{Al}_2\text{O}_3$ catalysts.

However, the acid strength on surface samples, the type of acid site absolutely plays a main role in deciding the performance of catalyst. It can be noticed from Table 4.4, both the concentration and the Brønsted/Lewis acid sites ratio boost obviously by increasing Pt on $\text{WO}_x/\gamma\text{-Al}_2\text{O}_3$ from 2%Pt to 5%Pt, further that it decrease. It suggesting that the excess Pt could be covered the surface of supported $\text{WO}_x/\gamma\text{-Al}_2\text{O}_3$ and Pt might be connected to a part of pore obstruct of supported acidic sites by Pt metals, which is inhibits the cooperation of ammonia molecules and the acidic sites. So the quantity of acid site was reduced when Pt content was reduced from 5% to 8% Pt [59].

Table 4.4 The amounts of Brønsted and Lewis acid sites over the catalysts with difference %Pt loading determined from the in situ DRIFTS of adsorbed NH₃

Catalyst	Lewis acid (a.u.) ^a	Brønsted acid (a.u.) ^a	Ratio B/L acidity
2%Pt/WO _x /γ-Al ₂ O ₃	4.4	14.6	3.31
5%Pt/WO _x /γ-Al ₂ O ₃	5.5	19.2	3.49
8%Pt/WO _x /γ-Al ₂ O ₃	1.2	5.9	4.91

^a The amount of acid sites were calculated from the quantity of the desorped ammonium from NH₃-IR.

Figure 4.10 showed the activity of glycerol hydrogenolysis over Pt/WO_x/γ-Al₂O₃ catalysts in varying Pt loading (2, 5, and 8 wt %).

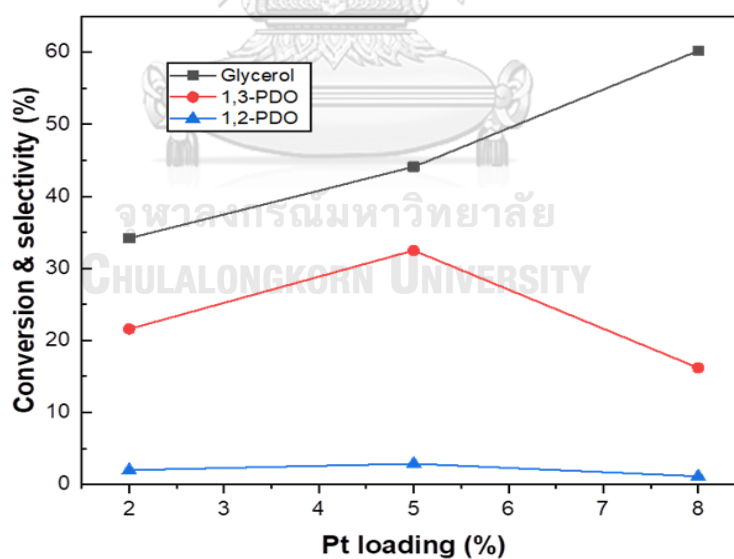


Figure 4.10 Effect of %Pt content on Glycerol Hydrogenolysis to 1,3-PDO.

As shown in Figure 4.10, the conversions of glycerol lift up from 34.7% to 60% accompanied by enhancing of Pt content from 2 to 8 wt% and the selectivity of 1,3-propanediol had the maximum value at 32.5% when the Pt content was 5 wt%. In addition, a substantial decrease in the selectivity of 1,2-propanediol was observed in an enhance in Pt loading amount. This result presents that the Brønsted acid sites not only are essential for the secondary hydroxyl dehydrated and also pretended to be benign for glycerol dehydrate to 3-HPA, which capable formed to 1,3-propanediol [53, 62]. According to the glycerol conversion was enhanced when Pt content higher, it show that platinum associated in the activation of the adsorbed glycerol reactant and then transformation to the intermediate in the later generated to the product [25]. All of the glycerol conversion, the 1,3-propanediol and the 1,2-propanediol selectivity developed with the improve of Pt content (2%Pt/WO_x/γ-Al₂O₃ to 5%Pt/WO_x/γ-Al₂O₃), that is related to the increase of the Brønsted and Lewis acid sites. It was indicated that Lewis acid sites are accountable for the glycerol dehydrated to acetol, which is hydrogenated acetol to form 1,2-propanediol over metal catalysts. And after the increasing of Pt loading to 8wt% on supported catalyst the glycerol conversion was enhanced but the 1,3-propanediol and 1,2-propanediol selectivity was decreased due to the diminished of the acidity as well. However, glycerol conversion does not show distinctly related to the dispersion of platinum, because the maximum values were not gained from the highest platinum dispersions.

4.4 Effect of tungsten oxide content to catalytic activity

4.4.1 IR spectra of pyridine adsorption

Pyridine-IR was presented to calculate the type of acid sites. As seen in Figure 4.11, the bands centred at ca. 1440 cm^{-1} was pyridine bands coordinated to Lewis sites [50]. The bands at ca. 1540 cm^{-1} was related to Brønsted acid sites. The adsorption around 1489 cm^{-1} was designed for the bonded of pyridine adsorb on Lewis and Brønsted acid sites [10]. The integration area of adsorption bands was estimated for the concentration of Lewis and Brønsted acid sites at ca. $1435\text{-}1445\text{ cm}^{-1}$ and $1535\text{-}1545\text{ cm}^{-1}$, respectively. As seen in Table 4.5, 2%Pt/ Al_2O_3 consumed part of Lewis acid sites, and it rarely obtained Brønsted acid sites. Adding of WO_x conducted a clearly improve in both Lewis and Brønsted acid sites. *Triwahyono et al.* indicated that Brønsted acid sites were came from hydroxyl groups connected on the covered or good dispersed WO_x of WO_3/ZrO_2 when Lewis acid sites were originated from the diminish of surface OH groups [63]. As a result, 2%Pt/10% $\text{WO}_x/\text{Al}_2\text{O}_3$ occurred while the surface of monolayer tungstate exposed and discovered the largest surface of WO_x .

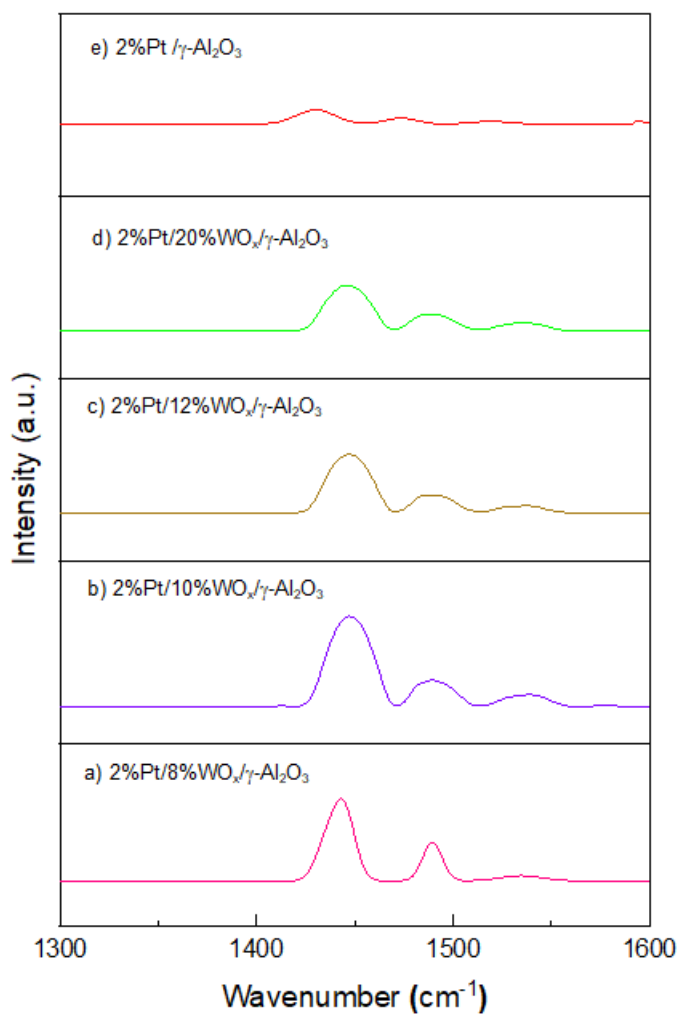


Figure 4.11 FTIR spectra of pyridine adsorption of 2%Pt/Al₂O₃ and 2%Pt/WO_x/Al₂O₃ with different tungsten loading catalysts

Table 4.5 Summarized the textural properties, acidities and the catalytic activity for 2%Pt/WO_x/ γ -Al₂O₃ with different tungsten content catalysts.

Catalyst	CO Absorbed ($\mu\text{mol CO/g cat}$)	Pt dispersion (%)	Conversion of glycerol (%)	Selectivity (%)			Lewis (a.u. / g cat.) ^a	Brønsted (a.u. / g cat.) ^a
				1,3- propanediol	1,2- propanediol	1,2- propanediol		
2%Pt/ γ -Al ₂ O ₃	26.4	13.2	26.4	n.d.	n.d.	0.3	0.23	
2%Pt/8%WO _x / γ -Al ₂ O ₃	50.4	25.2	34.6	21.6	2.1	1.61	0.56	
2%Pt/10%WO _x / γ -Al ₂ O ₃	58.2	29.1	40.1	28.3	3.1	2.52	1.23	
2%Pt/12%WO _x / γ -Al ₂ O ₃	51.4	25.7	38.1	26.8	2.6	2.21	1.01	
2%Pt/20%WO _x / γ -Al ₂ O ₃	46.2	23.1	35.0	23.4	2.3	2.16	0.98	

^a The amount of acid sites was calculated from the quantity of the desorbed pyridine from Py-IR.

Table 4.5 described the textural properties, acidities, the catalytic activity and the distributions of product for Pt/WO_x/γ-Al₂O₃ catalysts. The developing WO_x content up to 10 wt% was made Pt well dispersion, hinting that types of WO_x had an effect on the dispersion of Pt. However, a more improves in WO_x loading declined the dispersion mildly, which was may originated from part of hindrance of Pt particle by exaggeration of WO_x species. Similarly, the coverage effects were studied in ReO_x, SnO_x, and MoO_x catalyst. This might be described by the couple effects of WO_x activation, known as bimetallic coverage effect and dispersion effect. *Chen et al.* studied over Ru–MoO_x/ZrO₂ has proved that the existence of minor MoO_x species stimulates the dispersion of Ru metal, while surplus of MoO_x might be could impede the dispersion effect and cover of Ru site [64, 65]. For the conversion of glycerol, the Pt/γ-Al₂O₃ catalyst expressed the low activity; the conversion was rarely 26.4% and the selectivity of 1,3-propanediol and 1,2-propanediol were not detected. Against to Pt/WO_x/γ-Al₂O₃, glycerol conversion improved indeed for WO_x beneficial promoted catalysts. Relating to the selectivity, 1,3-propanediol selectivity on Pt/Al₂O₃ does not found. The other products were main degradation products acquired from consequential hydrogenolysis of propanediol [64]. Controversy, with the promotion of WO_x, it could be a considerably increased amount of 1,3-propanediol selectivity. From Table 4.5, the selectivity of 1,3-propanediol raise up to 21.6% over 2%Pt/8%WO_x/γ-Al₂O₃, whereas that of 1,2-propanediol rarely boost to a minor level (2.1%). The enhancing of 1,3-propanediol selectivity accompanied with increasing WO_x loading and attained a maximum at 10 wt% WO_x content. it is evident that 1,3-propanediol selectivity is relative to the concentration of Brønsted acid, indicating the favorable formation of 1,3-propanediol on Brønsted acid sites. From the literature [66], the WO_x structures on Pt/Al₂O₃ catalysts contained of monotungstate, polytungstate and WO₃ clusters, which up to the WO_x loading. Apparently, addition of WO_x to 10 wt%, it might be polytungstate species. Which essentially develop the amount of Brønsted acid sites, providing the greater 1,3-propanediol selectivity.

Nevertheless, more excessing in WO_x loading led to the mildly decline of selectivity due to the generation of crystalline WO_3 has a defected effect on the 1,3-propanediol selectivity due to The tungsten oxides cover on -OH groups of the γ -alumina, as the tungsten content increases , may describe the noticed decline in the glycerol conversion. Among the best reported results of the catalysts tested, 2%Pt/10% WO_x/γ - Al_2O_3 succeeded the good performance, up to 28.3% 1,3-propanediol selectivity, which was taken the reaction at mild condition. Taken together, the surplus of WO_x significantly not only built up glycerol conversion and also alternated the main product from 1,2-propanediol to 1,3-propanediol by switching the C-O compound.

4.5 Effect of pretreatment on catalytic activity

Figure 4.12 showed the natural of acidity sites and strength of the catalysts are relative to the product selectivity on hydrogenolysis of glycerol, which was generally characterized by the Py-IR. The Brønsted and Lewis acid sites were centered at 1535-1550 cm^{-1} and 1445-1460 cm^{-1} individually, and the concentration of the Brønsted acids and Lewis acids sites listed in Table 4.6 were calculated by the integration of the absorption peaks at 1535-1560 and 1435-1450 cm^{-1} , respectively. It was found that the reduced catalyst in H_2 atmosphere at 300°C after calcination at 300°C in air both of Brønsted acids and Lewis acids sites was decreased. As seen in Table 4.6

4.5.1 IR spectra of pyridine adsorption

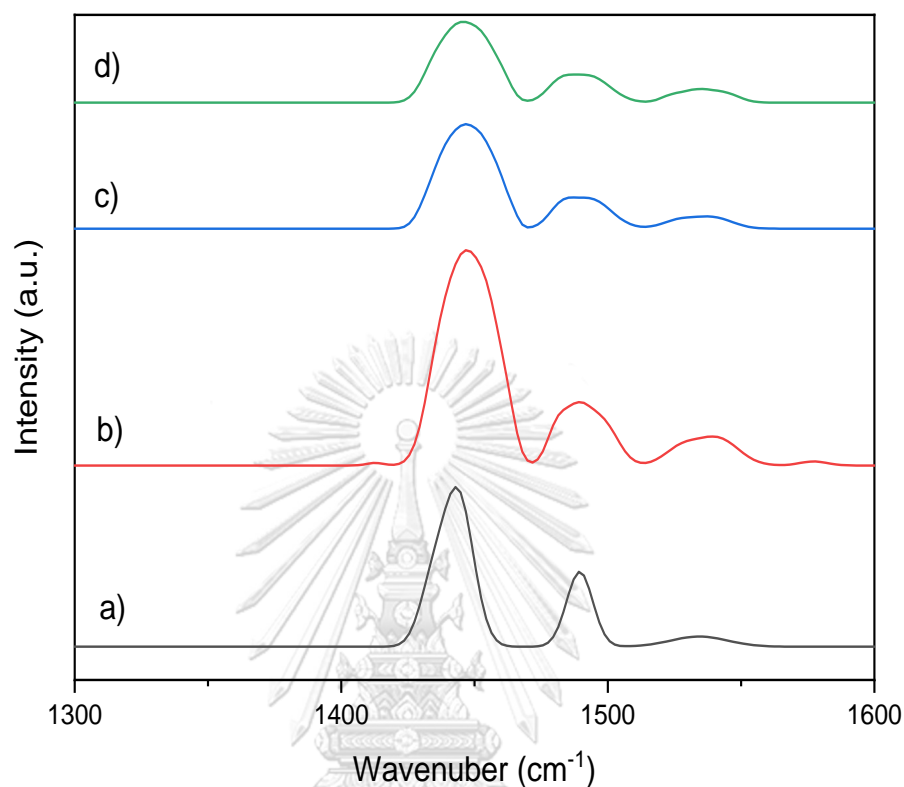


Figure 4.12 FTIR spectra of pyridine adsorption of a) 2%Pt/WO_x/Al₂O₃, b) 5%Pt/WO_x/Al₂O₃, and c) 2%Pt/WO_x/Al₂O₃ pretreat with H₂ at 300 °C and 5%Pt/WO_x/Al₂O₃ pretreat with H₂ at 300 °C catalysts

4.5.2 Temperature-programmed reduction of hydrogen (H₂-TPR)

The H₂-TPR profiles of the catalysts illustrated in Figure 4.13. H₂-TPD was studied in the temperature range (40-800°C), the supported alumina was not available to reduce. However, the successful reduction of WO_x/Al₂O₃ catalysts acquires the temperatures higher than 1100°C. The 5%Pt/WO_x/γ-Al₂O₃ catalysts TPR profile presents two major peaks at 280°C, which is referred to absolutely the reduction of PtO_x [67]. The presence of extending reduction peaks at 750 °C is apparently due to Pt^{δ+} species deeply cooperating with WO_x support [25]. Regarding the reduction of WO_x supported platinum catalyst; it initiated at a temperature

around 550°C. The H₂ spillover over the platinum metal approach to cover the WO_x surface, suggesting that H₂ species could approach on the oxides surface species [68].

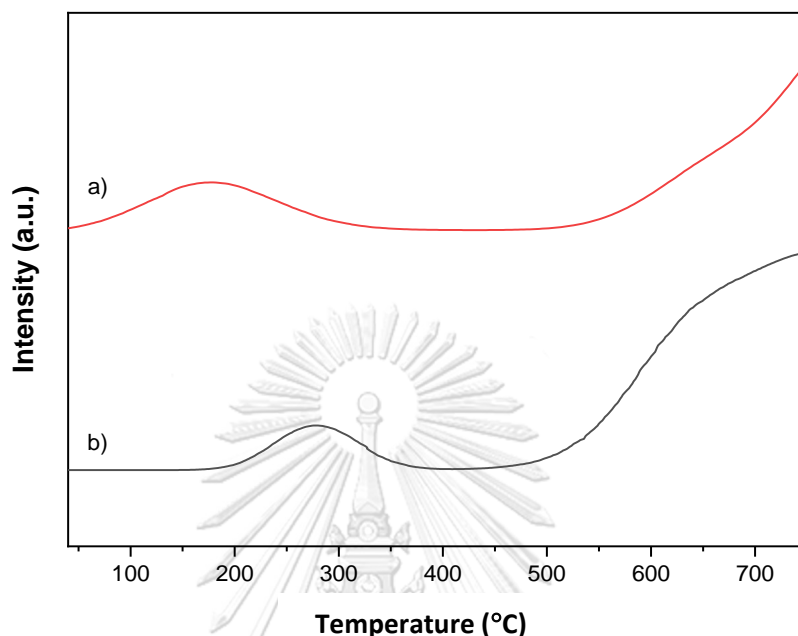


Figure 4.13 H₂-TPR profiles only observed on a). 2%Pt/WO_x/γ-Al₂O₃ and b). 5%Pt/WO_x/γ-Al₂O₃ catalysts

4.5.3 Temperature-programmed desorption of hydrogen (H₂-TPD)

Figure 4.14 showed the H₂-TPD profile of the reduced catalysts and fresh catalyst, it found that the centre of peak was shift to higher temperature than fresh catalysts. Normally, low temperature desorption peaks (< 200°C) are attributed to hydrogen desorbed from metallic of Pt particles. The high temperature desorption peaks (200–500°C) are denoted to hydrogen spill over to the surface support sites [69]. As studied in the literature [70], the desorption temperature was an index of the H-metal interaction and the peak area was that of metal disclosure and adsorption quantity. Thus, the peak around 200-500°C were designed to the concentration of hydrogen spill-over on the metal oxide catalysts. From the H₂-TPD results, it is clearly that these the pre-treated catalysts could be generated more hydrogen species than non-pretreated catalyst. The amounts of hydrogen uptake on catalysts by H₂-TPD

test were also evaluated from the integration of peak areas and are shown in Table 4.6 and only observed on 5%Pt loading. The total amounts of hydrogen adsorbed on the surfaced of reduced catalysts were higher than fresh catalysts. It is indicated that the spill-over of hydrogen molecules from the Pt metal on $\text{WO}_x/\gamma\text{-Al}_2\text{O}_3$ supported catalysts occurred after catalyst was reduced in H_2 atmosphere.

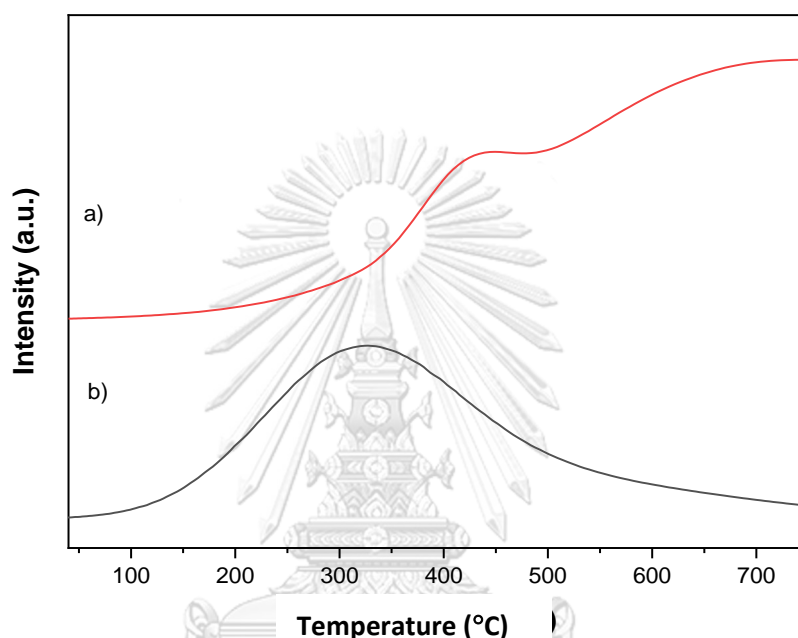


Figure 4.14 H_2 -TPD profiles of the catalysts; only observed catalysts

a) 5%Pt/ $\text{WO}_x/\gamma\text{-Al}_2\text{O}_3$ pretreated with H_2 at 300°C and b) 5%Pt/ $\text{WO}_x/\gamma\text{-Al}_2\text{O}_3$ catalysts

4.5.4 X-ray absorption spectroscopy (XAS)

Figure 4.15 showed the normalized X-ray absorption near-edge structure (XANES) spectra of the sample catalysts 2%Pt/ $\text{WO}_x/\gamma\text{-Al}_2\text{O}_3$, 2%Pt/ $\text{WO}_x/\gamma\text{-Al}_2\text{O}_3$ reduced catalyst and 2%Pt/ $\text{WO}_x/\gamma\text{-Al}_2\text{O}_3$ used catalyst together with spectra of the Pt foil, K_2PtCl_4 and PtO_2 .

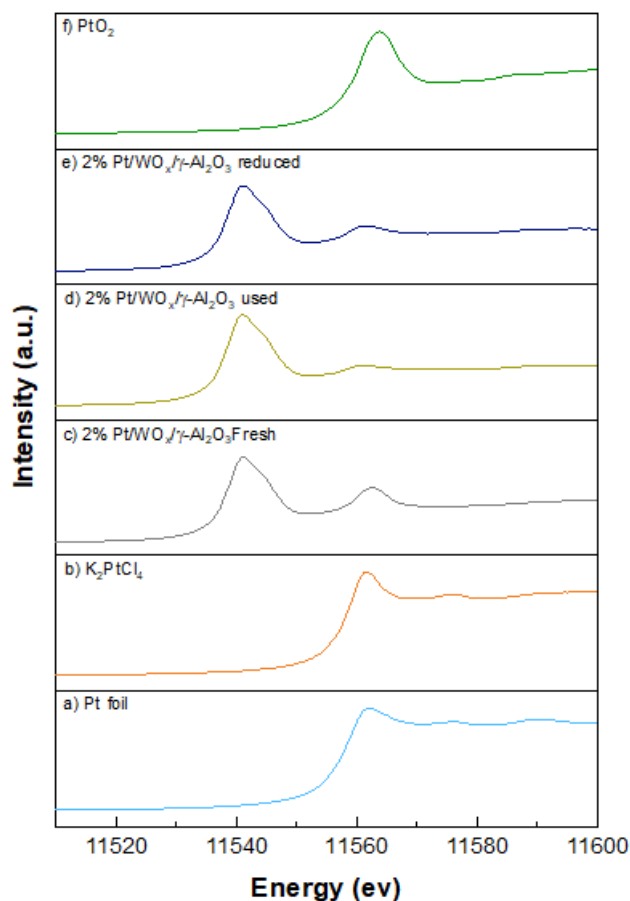


Figure 4.15 Pt L3-edge XANES spectra of 2%Pt/WO_x/γ-Al₂O₃ catalysts.

As seen in Figure 4.15, the first peak at 11562 eV corresponds to the pre-edge of 2%Pt/WO_x/γ-Al₂O₃ catalysts, which is close to that of PtO₂ and K₂PtCl₄, reflecting that the Pt in sample 2%Pt/WO_x/γ-Al₂O₃ exists as Pt^{δ+}. Next, the peak referred to the white-line intensity of 2%Pt/WO_x/γ-Al₂O₃ reduced and used catalyst is lower than that of 2%Pt/WO_x/γ-Al₂O₃ sample, and almost similar to the Pt foil, which suggests that the dominance of the Pt⁰ particles. There was a minor shift in the edge position for the used catalyst and reduced catalyst, suggests that there was a change in the state of Pt to other formation [71].

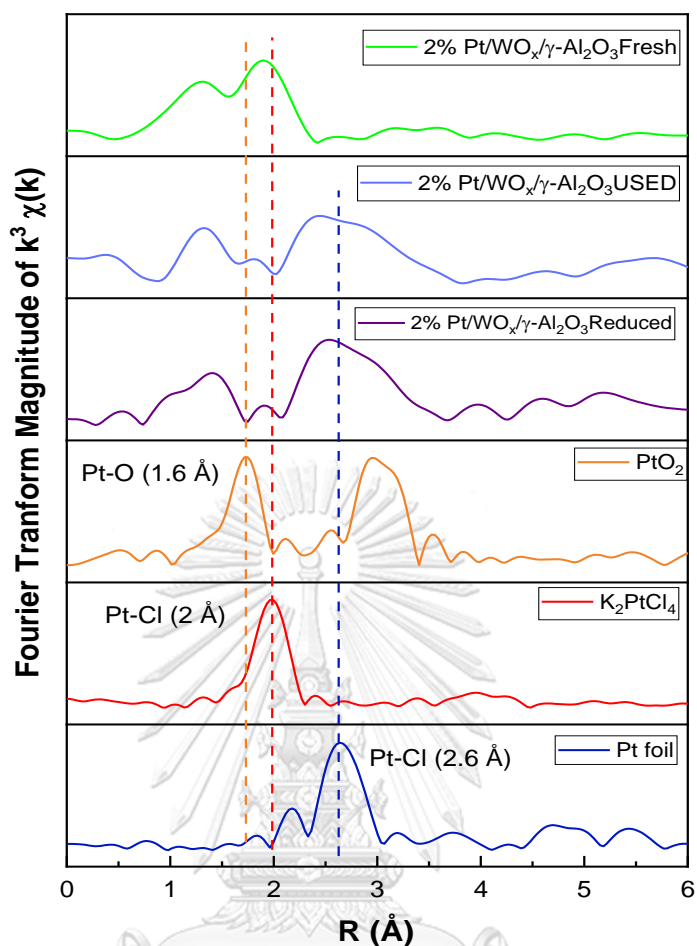


Figure 4.16 The K^3 -weighted Fourier transform spectra from EXAFS of catalysts.

Figure 4.16 illustrated the FT for 2%Pt/WO_x/γ-Al₂O₃ (fresh, reduced and used catalyst) and reference compound. The FT of PtO₂ had similar oscillations to those of 2%Pt/WO_x/γ-Al₂O₃, which reflect that the structure of Pt in 2%Pt/WO_x/γ-Al₂O₃ fresh catalyst was Pt bonded with oxygen. The peak at 1–2 Å for the 2%Pt/WO_x/γ-Al₂O₃ fresh catalyst corresponded to Pt–O and there was weak intensities peak at 3 Å implying Pt well disperse over surface support, while the peaks in the range of 2–3 Å can be defined to Pt–Cl and Pt–Pt. For 2%Pt/WO_x/γ-Al₂O₃ used and reduced catalysts had same oscillations to those of Pt–Pt suggesting that Pt^{δ+} change to Pt⁰ in well agreement with Pt L3-edge XANES spectra result. Besides, the peak intensities in the range of 2.5–4 Å decreased. The lower peak intensities for the catalysts illustrate

that their Pt–Pt were lower and smaller in coordination numbers (CNs) and particle sizes, respectively. [72].

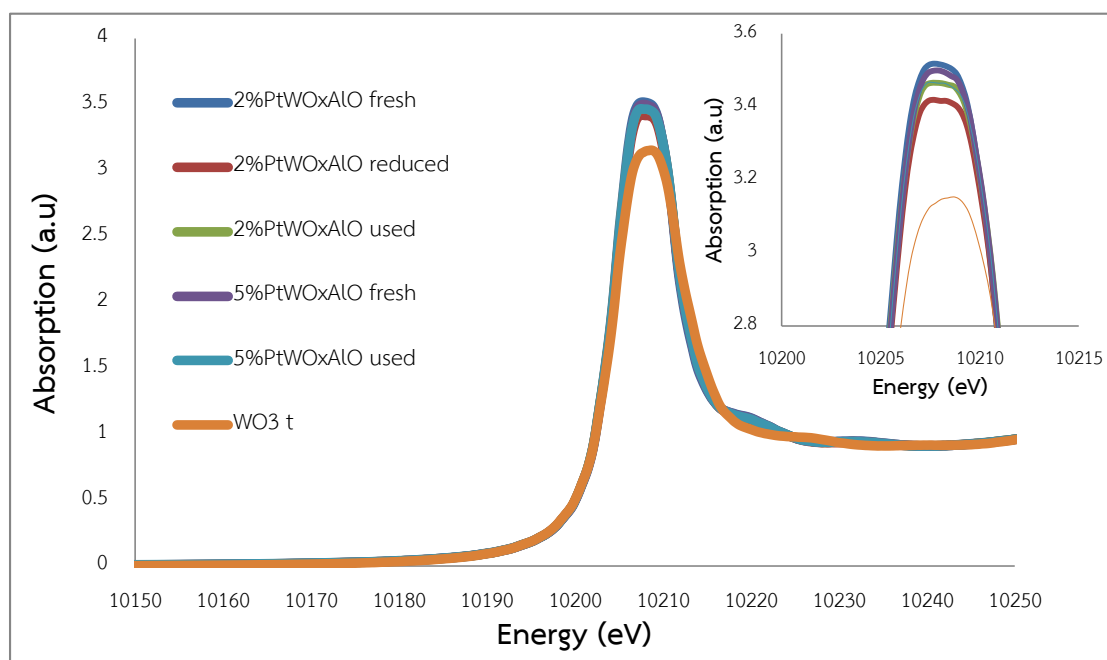


Figure 4.17 W L3-edge XANES spectra of catalysts.

Figure 4.17 showed W L3 edge XANES spectra for the Pt/WO_x/γ-Al₂O₃ sample and reference catalysts. Compared with the W L3 edge XANES spectra for WO₃, all of the catalysts have a similar structure to that of WO₃. Even though the absorption edge structure was comparable, there was a minor decrease in intensities after reaction and reduction process under H₂ atmosphere at high temperature.

The glycerol conversion and the selectivity of the main products of pretreated and non-pretreated catalysts in glycerol hydrogenolysis are summarized in Table 4.6. It was found that the glycerol conversion of non-pretreated catalysts was better than pretreated catalyst because the active sites reduced after the pretreatment catalyst with H₂. This may be associated to the evidence that some Pt metal were enclosed or exposed by the metallic oxides immigrated from the support, introducing to the decreasing of the CO adsorption concentration [53], and the selectivity of 1,3 and 1,2-propanediol of the pretreatment catalyst also lower.

The result had the same in 2%Pt and 5% Pt loading on $\text{WO}_x/\text{Al}_2\text{O}_3$ support. As seen in Table 4.6, the glycerol conversion of 2%Pt/ $\text{WO}_x/\gamma\text{-Al}_2\text{O}_3$ decrease from 34.6 % to 21.4 % after the reduction process of catalyst. For the selectivity of 1,3 and 1,2-propanediol also decreased (from 21.6% to 15.2% and 4.1% to 1.5%, respectively). Suggesting that, it might be due to the Brønsted and Lewis acid site was declined after reduced catalyst with H_2 pressure at 300 °C. Hence, the nature of the acid site has an important role in determining the product distribution. Brønsted acid site remove the middle -OH group of glycerol to generate 1,3-propanediol and Lewis acid sites favor forming 1,2-propanediol. As reported in many of the literature [21, 22, 58]. From the H_2 -TPD results, it is indicated that 5%Pt/ $\text{WO}_x/\gamma\text{-Al}_2\text{O}_3$ pretreatment catalyst generated more H_2 spillover, which led to high selectivity of by-product (1-PO and gas) and its selectivity was increased from 30.9% from 50.3% compared with 5%Pt/ $\text{WO}_x/\gamma\text{-Al}_2\text{O}_3$ (non-pretreated).

Table 4.6 Catalytic performance of glycerol hydrogenolysis over x%Pt/WO_x/γ-Al₂O₃ pretreated and non-pretreated catalysts

Catalyst	CO Absorbed (μmol CO/ g cat)	Conversion of glycerol (%)	Selectivity (%)				Lewis (a.u.)	Brønsted (a.u.)	H ₂ Absorbed (μmol H ₂ / g cat)
			1,3-propanediol	1,2-propanediol	1-PO				
2%Pt/WO _x /γ-Al ₂ O ₃	50.4	34.6	21.6	4.1	44.8	5.98	0.89	N.A.	
2%Pt/WO _x /γ-Al ₂ O ₃ Reduced 300 °C	18.1	21.7	15.2	1.5	35.9	3.16	0.22	N.A.	
5%Pt/WO _x /γ-Al ₂ O ₃	103.8	44.1	32.5	2.9	50.3	6.51	1.41	47.7	
5%Pt/WO _x /γ-Al ₂ O ₃ Reduced 300 °C	70.4	31.8	13.6	0.9	30.5	4.26	0.92	112.2	

CHAPTER IV

CONCLUSION AND RECOMMENDATIONS

5.1 Conclusion

The catalytic activity for hydrogenolysis of glycerol was compared between AlOOH and $\gamma\text{-Al}_2\text{O}_3$. It was found that, the glycerol conversion and 1,3-propanediol selectivity of $2\% \text{Pt}/\text{WO}_x/\gamma\text{-Al}_2\text{O}_3$ higher than $2\% \text{Pt}/\text{WO}_x/\text{AlOOH}$ because the increasing of dispersion of Pt, total acidities, and amount of Brønsted and Lewis acid sites after the enhance of calcination support temperature from $800\text{ }^\circ\text{C}$ to $900\text{ }^\circ\text{C}$.

According to the result, The Brønsted acidities play a significant role to generate 1,3-propanediol selectivity, providing direct prove that Brønsted acid sites possible to break secondary C-O of glycerol to form 1,3-propanediol. The reduction process impacted the activity of glycerol hydrogenolysis significantly, demonstrating that a Brønsted acidities and active site of the pretreated catalyst decrease, led to the decreasing of glycerol conversion and selectivity of 1,3-propanediol. Moreover, an effect of H_2 -spillover also influences over hydrogenolysis of glycerol to generated by-product derived from the metal of reduced catalyst.

5.2 Recommendation

5.2.1 The effect of catalyst pretreatment to Brønsted acid site should be more investigated.

5.2.2 The influence of H_2 -spillover and Brønsted acid site which one play significant role to produced by-product should be studied.

REFERENCES

- [1] Renewable Energy Policy Network for the 21st Century Renewables 2017 global status report 2017. Available from: http://www.ren21.net/wp-content/uploads/2017/06/17-8399_GSR_2017_Full_Report_0621_Opt.pdf [2017, September 5]
- [2] OECD FAO Agricultural Outlook OECD Publishing 2013. Available from: http://dx.doi.org/10.1787/agr_outlook-2013-en
- [3] Lima, C.J.A.M.B.P.P.A.L.d. Glycerol: a versatile renewable feedstock for the chemical industry. Brazil: Springer, 2017.
- [4] De Lima, A.L., Ronconi, C.M., and Mota, C.J.A. Heterogeneous basic catalysts for biodiesel production. Catalysis Science & Technology 6(9) (2016): 2877-2891.
- [5] 4 - Biodiesel Production. in Knothe, G., Krahl, J., and Van Gerpen, J. (eds.), The Biodiesel Handbook (Second Edition), pp. 31-96: AOCS Press, 2010.
- [6] Monteiro, M.R., Kugelmeier, C.L., Pinheiro, R.S., Batalha, M.O., and da Silva César, A. Glycerol from biodiesel production: Technological paths for sustainability. Renewable and Sustainable Energy Reviews 88 (2018): 109-122.
- [7] Don W. Green, R.H.P. Perry's Chemical Engineers' Handbook. Eighth ed.: McGraw-Hill, 2008.
- [8] Haworth, D.D. General Chemistry: Principles and Structure, Fifth Edition (Brady, James E.). Journal of Chemical Education 67(7) (1990): A196.
- [9] Centi, G. and van Santen, R.A. Catalysis for renewables: from feedstock to energy production. John Wiley & Sons, 2008.
- [10] Singhabhandhu, A. and Tezuka, T. A perspective on incorporation of glycerin purification process in biodiesel plants using waste cooking oil as feedstock. Energy 35(6) (2010): 2493-2504.
- [11] Tan, H., Aziz, A.A., and Aroua, M. Glycerol production and its applications as a raw material: A review. Renewable and Sustainable Energy Reviews 27 (2013): 118-127.
- [12] Katryniok, B., Paul, S., Bellière-Baca, V., Rey, P., and Dumeignil, F. Glycerol

- dehydration to acrolein in the context of new uses of glycerol. Green Chemistry 12(12) (2010): 2079-2098.
- [13] Johnson, D.T. and Taconi, K.A. The glycerin glut: Options for the value-added conversion of crude glycerol resulting from biodiesel production. Environmental Progress 26(4) (2007): 338-348.
- [14] Bagheri, S., Julkapli, N.M., and Yehye, W.A. Catalytic conversion of biodiesel derived raw glycerol to value added products. Renewable and Sustainable Energy Reviews 41 (2015): 113-127.
- [15] Anitha, M., Kamarudin, S.K., and Kofli, N.T. The potential of glycerol as a value-added commodity. Chemical Engineering Journal 295 (2016): 119-130.
- [16] Lee, C., Aroua, M., Daud, W., Cognet, P., Pérès-Lucchese, Y., Fabre, P., *et al.* A review: conversion of bioglycerol into 1, 3-propanediol via biological and chemical method. Renewable and Sustainable Energy Reviews 42 (2015): 963-972.
- [17] Ardila, A.N., Sánchez-Castillo, M.A., Zepeda, T.A., Villa, A.L., and Fuentes, G.A. Glycerol hydrodeoxygenation to 1, 2-propanediol catalyzed by CuPd/TiO₂-Na. Applied Catalysis B: Environmental 219 (2017): 658-671.
- [18] Dieuzeide, M.L., de Urtiaga, R., Jobbagy, M., and Amadeo, N. Vapor phase hydrogenolysis of glycerol to 1, 2-propanediol at atmospheric pressure over copper catalysts supported on mesoporous alumina. Catalysis Today 296 (2017): 19-25.
- [19] Schlaf, M. Selective deoxygenation of sugar polyols to α , ω -diols and other oxygen content reduced materials—A new challenge to homogeneous ionic hydrogenation and hydrogenolysis catalysis. Dalton Transactions (39) (2006): 4645-4653.
- [20] Nakagawa, Y., Tamura, M., and Tomishige, K. Catalytic materials for the hydrogenolysis of glycerol to 1, 3-propanediol. Journal of Materials Chemistry A 2(19) (2014): 6688-6702.
- [21] Wang, Y., Zhou, J., and Guo, X. Catalytic hydrogenolysis of glycerol to propanediols: a review. RSC Advances 5(91) (2015): 74611-74628.

- [22] Amada, Y., Shinmi, Y., Koso, S., Kubota, T., Nakagawa, Y., and Tomishige, K. Reaction mechanism of the glycerol hydrogenolysis to 1, 3-propanediol over Ir–ReO_x/SiO₂ catalyst. Applied Catalysis B: Environmental 105(1-2) (2011): 117-127.
- [23] Ten Dam, J. and Hanefeld, U. Renewable chemicals: dehydroxylation of glycerol and polyols. ChemSusChem 4(8) (2011): 1017-1034.
- [24] Nakagawa, Y. and Tomishige, K. Heterogeneous catalysis of the glycerol hydrogenolysis. Catalysis Science & Technology 1(2) (2011): 179-190.
- [25] García-Fernández, S., Gandarias, I., Requies, J., Güemez, M.B., Bennici, S., Auroux, A., *et al.* New approaches to the Pt/WO_x/Al₂O₃ catalytic system behavior for the selective glycerol hydrogenolysis to 1,3-propanediol. Journal of Catalysis 323 (2015): 65-75.
- [26] Montassier, C., Giraud, D., Barbier, J., and Boitiaux, J. Polyol transformation by liquid-phase heterogeneous catalysis over metals. Bulletin de la société chimique de France (2) (1989): 148-155.
- [27] Montassier, C., Menezes, J., Hoang, L., Renaud, C., and Barbier, J. Aqueous polyol conversions on ruthenium and on sulfur-modified ruthenium. Journal of Molecular Catalysis 70(1) (1991): 99-110.
- [28] Montassier, C., Ménézo, J., Moukolo, J., Naja, J., Hoang, L., Barbier, J., *et al.* Polyol conversions into furanic derivatives on bimetallic catalysts: Cu-Ru, Cu-Pt and Ru-Cu. Journal of Molecular Catalysis 70(1) (1991): 65-84.
- [29] Lahr, D.G. and Shanks, B.H. Kinetic analysis of the hydrogenolysis of lower polyhydric alcohols: glycerol to glycols. Industrial & engineering chemistry research 42(22) (2003): 5467-5472.
- [30] Lahr, D.G. and Shanks, B.H. Effect of sulfur and temperature on ruthenium-catalyzed glycerol hydrogenolysis to glycols. Journal of Catalysis 232(2) (2005): 386-394.
- [31] Maris, E.P., Ketchie, W.C., Murayama, M., and Davis, R.J. Glycerol hydrogenolysis on carbon-supported PtRu and AuRu bimetallic catalysts. Journal of Catalysis 251(2) (2007): 281-294.
- [32] Dasari, M.A., Kiatsimkul, P.-P., Sutterlin, W.R., and Suppes, G.J. Low-pressure hydrogenolysis of glycerol to propylene glycol. Applied Catalysis A: General

- 281(1-2) (2005): 225-231.
- [33] Furikado, I., Miyazawa, T., Koso, S., Shima, A., Kunimori, K., and Tomishige, K. Catalytic performance of Rh/SiO₂ in glycerol reaction under hydrogen. Green Chemistry 9(6) (2007): 582-588.
- [34] Kim, N.D., Park, J.R., Park, D.S., Kwak, B.K., and Yi, J. Promoter effect of Pd in CuCr₂O₄ catalysts on the hydrogenolysis of glycerol to 1, 2-propanediol. Green Chemistry 14(9) (2012): 2638-2646.
- [35] Balaraju, M., Rekha, V., Prasad, P.S., Prasad, R., and Lingaiah, N. Selective hydrogenolysis of glycerol to 1, 2-propanediol over Cu-ZnO catalysts. Catalysis Letters 126(1-2) (2008): 119-124.
- [36] Balaraju, M., Jagadeeswaraiyah, K., Prasad, P.S., and Lingaiah, N. Catalytic hydrogenolysis of biodiesel derived glycerol to 1, 2-propanediol over Cu-MgO catalysts. Catalysis Science & Technology 2(9) (2012): 1967-1976.
- [37] Yuan, Z., Wang, J., Wang, L., Xie, W., Chen, P., Hou, Z., *et al.* Biodiesel derived glycerol hydrogenolysis to 1, 2-propanediol on Cu/MgO catalysts. Bioresource Technology 101(18) (2010): 7088-7092.
- [38] Durán-Martín, D., Ojeda, M., Granados, M.L., Fierro, J., and Mariscal, R. Stability and regeneration of Cu-ZrO₂ catalysts used in glycerol hydrogenolysis to 1, 2-propanediol. Catalysis Today 210 (2013): 98-105.
- [39] Mane, R., Kondawar, S., Niphadkar, P., Joshi, P., Patil, K., and Rode, C. Effect of preparation parameters of Cu catalysts on their physico-chemical properties and activities for glycerol hydrogenolysis. Catalysis Today 198(1) (2012): 321-329.
- [40] Wolosiak-Hnat, A., Milchert, E., and Grzmil, B. Influence of parameters on glycerol hydrogenolysis over a Cu/Al₂O₃ catalyst. Chemical Engineering & Technology 36(3) (2013): 411-418.
- [41] Nakagawa, Y., Shinmi, Y., Koso, S., and Tomishige, K. Direct hydrogenolysis of glycerol into 1, 3-propanediol over rhenium-modified iridium catalyst. Journal of Catalysis 272(2) (2010): 191-194.
- [42] Shinmi, Y., Koso, S., Kubota, T., Nakagawa, Y., and Tomishige, K. Modification of Rh/SiO₂ catalyst for the hydrogenolysis of glycerol in water. Applied Catalysis B:

- Environmental 94(3-4) (2010): 318-326.
- [43] Chia, M., Pagán-Torres, Y.J., Hibbitts, D., Tan, Q., Pham, H.N., Datye, A.K., *et al.* Selective hydrogenolysis of polyols and cyclic ethers over bifunctional surface sites on rhodium–rhenium catalysts. Journal of the American Chemical Society 133(32) (2011): 12675-12689.
- [44] Longjie, L., ZHANG, Y., Aiqin, W., and ZHANG, T. Mesoporous WO₃ supported Pt catalyst for hydrogenolysis of glycerol to 1, 3-propanediol. Chinese Journal of Catalysis 33(7-8) (2012): 1257-1261.
- [45] Arundhathi, R., Mizugaki, T., Mitsudome, T., Jitsukawa, K., and Kaneda, K. Highly Selective Hydrogenolysis of Glycerol to 1,3-Propanediol over a Boehmite-Supported Platinum/Tungsten Catalyst. ChemSusChem 6(8) (2013): 1345-1347.
- [46] García-Fernández, S., Gandarias, I., Requies, J., Soulimani, F., Arias, P.L., and Weckhuysen, B.M. The role of tungsten oxide in the selective hydrogenolysis of glycerol to 1, 3-propanediol over Pt/WO_x/Al₂O₃. Applied Catalysis B: Environmental 204 (2017): 260-272.
- [47] Front Matter for Volume 882. AIP Conference Proceedings 882(1) (2007): frontmatter.
- [48] Iwasawa, Y. FRONT MATTER. in X-Ray Absorption Fine Structure for Catalysts and Surfaces, pp. i-xvi.
- [49] Asakura, K. Polarization-dependent total reflection fluorescence extended X-ray absorption fine structure and its application to supported catalysis. in Catalysis: Volume 24, pp. 281-322: The Royal Society of Chemistry, 2012.
- [50] Zhu, S., Gao, X., Zhu, Y., and Li, Y. Promoting effect of WO_x on selective hydrogenolysis of glycerol to 1,3-propanediol over bifunctional Pt–WO_x/Al₂O₃ catalysts. Journal of Molecular Catalysis A: Chemical 398 (2015): 391-398.
- [51] Jiang, Z.Q., Ma, H.W., Yang, J., and Wang, L. Synthesis of Nanosized Pseudoboehmite and γ -Al₂O₃ by Control Precipitation Method. in Advanced Materials Research, pp. 46-52: Trans Tech Publ, 2013.
- [52] Barton, D.G., Soled, S.L., and Iglesia, E. Solid acid catalysts based on supported tungsten oxides. Topics in Catalysis 6(1-4) (1998): 87-99.

- [53] Feng, S., Zhao, B., Liu, L., and Dong, J. Platinum Supported on WO₃-Doped Aluminosilicate: A Highly Efficient Catalyst for Selective Hydrogenolysis of Glycerol to 1,3-Propanediol. Industrial & engineering chemistry research 56(39) (2017): 11065-11074.
- [54] Wu, X., Zhang, L., Weng, D., Liu, S., Si, Z., and Fan, J. Total oxidation of propane on Pt/WO_x/Al₂O₃ catalysts by formation of metastable Pt^{δ+} species interacted with WO_x clusters. J Hazard Mater 225-226 (2012): 146-54.
- [55] Del Nero, M., Galindo, C., Barillon, R., Halter, E., and Madé, B. Surface reactivity of α -Al₂O₃ and mechanisms of phosphate sorption: In situ ATR-FTIR spectroscopy and ζ potential studies. Journal of Colloid and Interface Science 342(2) (2010): 437-444.
- [56] Qin, L.-Z., Song, M.-J., and Chen, C.-L. Aqueous-phase deoxygenation of glycerol to 1,3-propanediol over Pt/WO₃/ZrO₂ catalysts in a fixed-bed reactor. Green Chemistry 12(8) (2010): 1466-1472.
- [57] Zhu, S., Qiu, Y., Zhu, Y., Hao, S., Zheng, H., and Li, Y. Hydrogenolysis of glycerol to 1, 3-propanediol over bifunctional catalysts containing Pt and heteropolyacids. Catalysis Today 212 (2013): 120-126.
- [58] Zhu, S., Zhu, Y., Hao, S., Chen, L., Zhang, B., and Li, Y. Aqueous-Phase Hydrogenolysis of Glycerol to 1,3-propanediol Over Pt-H₄SiW₁₂O₄₀/SiO₂. Catalysis Letters 142(2) (2012): 267-274.
- [59] Priya, S.S., Bhanuchander, P., Kumar, V.P., Dumbre, D.K., Periasamy, S.R., Bhargava, S.K., *et al.* Platinum Supported on H-Mordenite: A Highly Efficient Catalyst for Selective Hydrogenolysis of Glycerol to 1,3-Propanediol. ACS Sustainable Chemistry & Engineering 4(3) (2016): 1212-1222.
- [60] Cornaglia, L., Houalla, M., Goldwasser, J., and Hercules, D.M. Determination of the surface coverage of Re/Al₂O₃ catalysts by ion scattering spectroscopy and low-temperature CO adsorption. Catalysis Letters 63(3) (1999): 131-133.
- [61] Karakonstantis, L., Bourikas, K., and Lycourghiotis, A. Tungsten-Oxo-Species Deposited on Alumina. I. Investigation of the Nature of the Tungstates Deposited on the Interface of the γ -Alumina/Electrolyte Solutions at Various pH's. Journal

- of Catalysis 162(2) (1996): 295-305.
- [62] Gong, L., Lu, Y., Ding, Y., Lin, R., Li, J., Dong, W., *et al.* Selective hydrogenolysis of glycerol to 1,3-propanediol over a Pt/WO₃/TiO₂/SiO₂ catalyst in aqueous media. Applied Catalysis A: General 390(1) (2010): 119-126.
- [63] Triwahyono, S., Yamada, T., and Hattori, H. IR study of acid sites on WO₃-ZrO₂ and Pt/WO₃-ZrO₂. Applied Catalysis A: General 242(1) (2003): 101-109.
- [64] Gandarias, I., Arias, P.L., Requies, J., Güemez, M.B., and Fierro, J.L.G. Hydrogenolysis of glycerol to propanediols over a Pt/ASA catalyst: The role of acid and metal sites on product selectivity and the reaction mechanism. Vol. 97, 2010.
- [65] Chen, L., Zhu, Y., Zheng, H., Zhang, C., and Li, Y.-W. Aqueous-phase hydrodeoxygenation of propanoic acid over the Ru/ZrO₂ and Ru-Mo/ZrO₂ catalysts. 411-412 (2012): 95-104.
- [66] Calabro, D., Vartuli, J., and Santiesteban, J. The characterization of tungsten-oxide-modified zirconia supports for dual functional catalysis. Topics in Catalysis 18(3-4) (2002): 231-242.
- [67] Contreras, J.L., Fuentes, G.A., Zeifert, B., and Salmones, J. Stabilization of supported platinum nanoparticles on γ -alumina catalysts by addition of tungsten. Journal of Alloys and Compounds 483(1) (2009): 371-373.
- [68] Guntida, A., Suriye, K., Panpranot, J., and Praserthdam, P. Comparative Study of Lewis Acid Transformation on Non-reducible and Reducible Oxides Under Hydrogen Atmosphere by In Situ DRIFTS of Adsorbed NH₃. Topics in Catalysis 61(15) (2018): 1641-1652.
- [69] Paál, Z. and Menon, P.G. Hydrogen Effects in Metal Catalysts. Catalysis Reviews 25(2) (1983): 229-324.
- [70] Liu, C., Li, X., and Wang, T. Catalytic hydrogenation of isophthalonitrile (IPN) over supported monometallic and bimetallic catalysts. RSC Advances 5(71) (2015): 57277-57285.
- [71] Murata, N., Suzuki, T., Kobayashi, M., Togoh, F., and Asakura, K. Characterization of Pt-doped SnO₂ catalyst for a high-performance micro gas sensor. Physical

chemistry chemical physics 15(41) (2013): 17938-17946.

- [72] Yiqiu, F., Cheng, S., Wang, H., Ye, D., Xie, S., Pei, Y., *et al.* Nanoparticulate Pt on mesoporous SBA-15 doped with extremely low amount of W as highly selective catalyst for glycerol hydrogenolysis to 1,3-propanediol. Green Chemistry 19 (2017).





APPENDIX

จุฬาลงกรณ์มหาวิทยาลัย
CHULALONGKORN UNIVERSITY

APPENDIX A

CALIBRATION CURVES

Calibration curves were done from gas chromatography (Shimadzu GC-14B) with the operating conditions as mentioned in Table 3.1. The gas and liquid standard were injected into gas chromatography at different concentrations. Peak area for each concentration was analyzed from gas chromatography. Then, calibration curves were plotted between peak area and mole of the sample injected into gas chromatography. Figure A.1 – Figure A.5 presented the calibration curves for glycerol, 1-3-propanediol, 1-2-propanediol, Ethanol and 1-propanol, respectively.

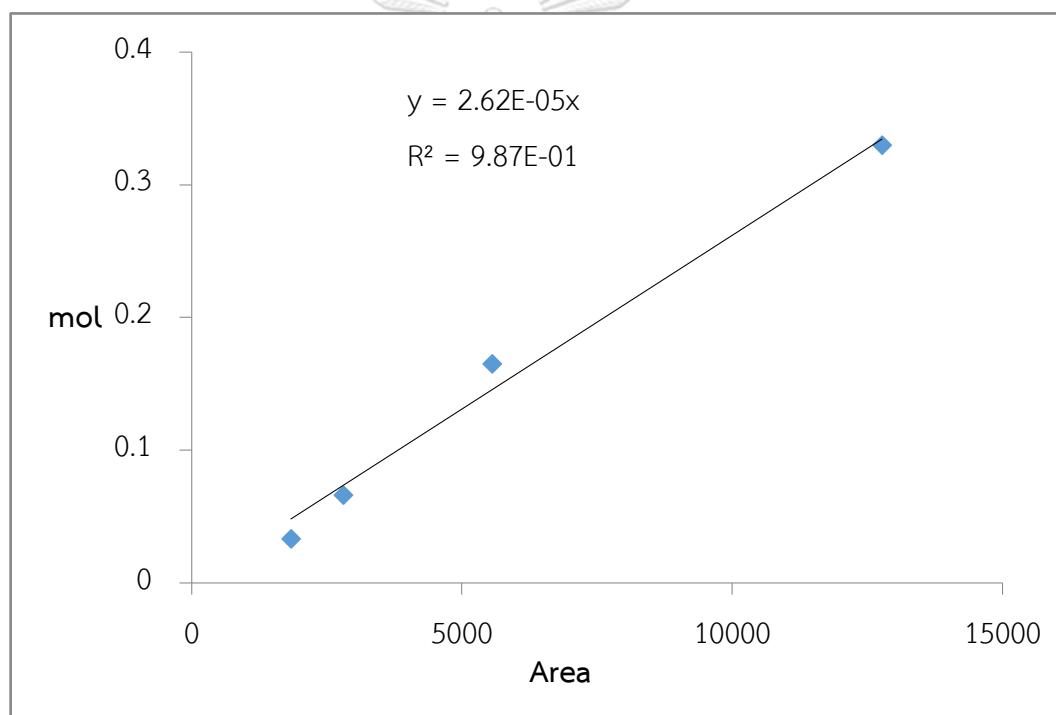


Figure A.1 Calibration curve of Glycerol

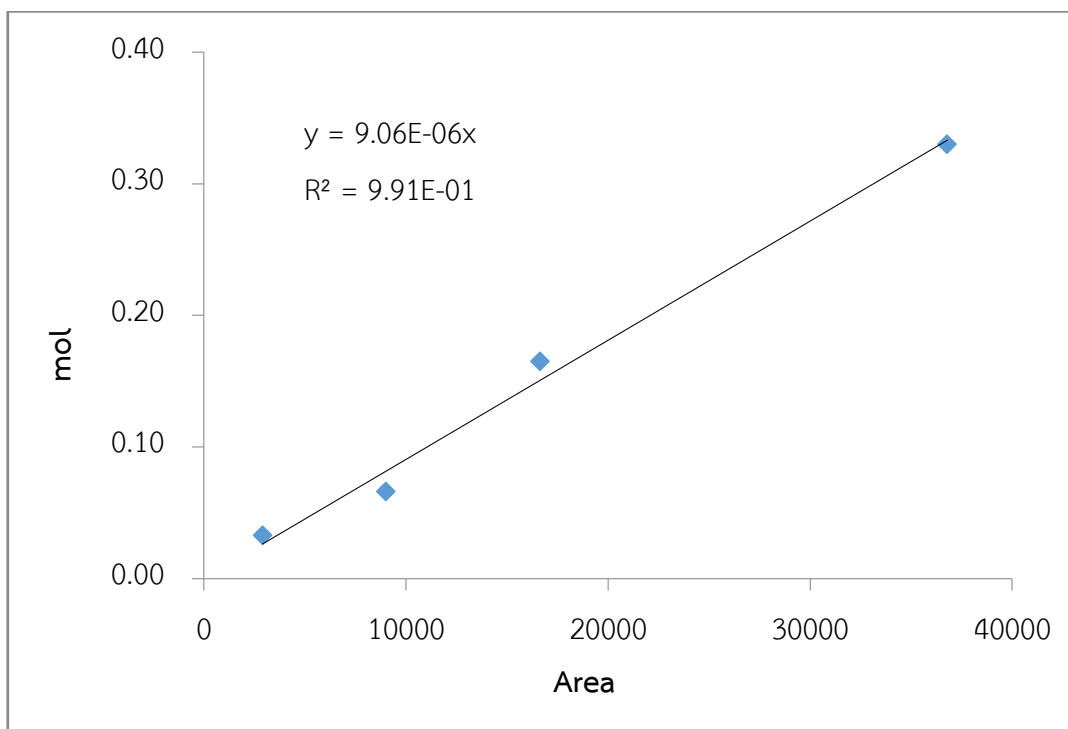


Figure A.2 Calibration curve of 1,3-propanediol

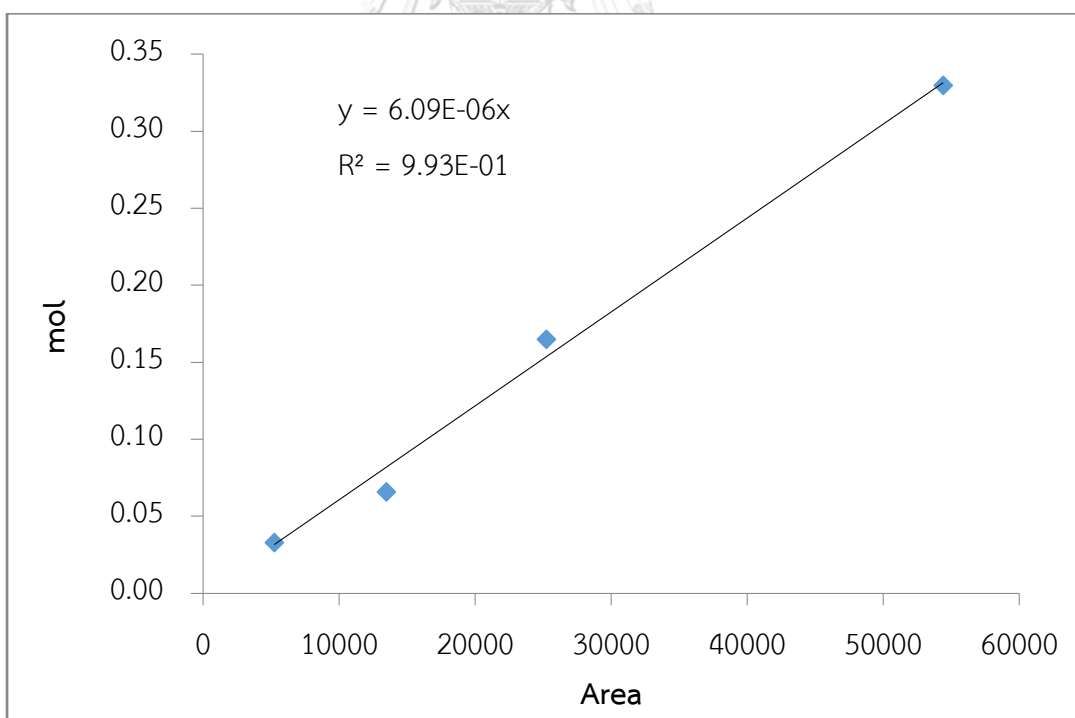


Figure A.3 Calibration curve of 1,2-propanediol

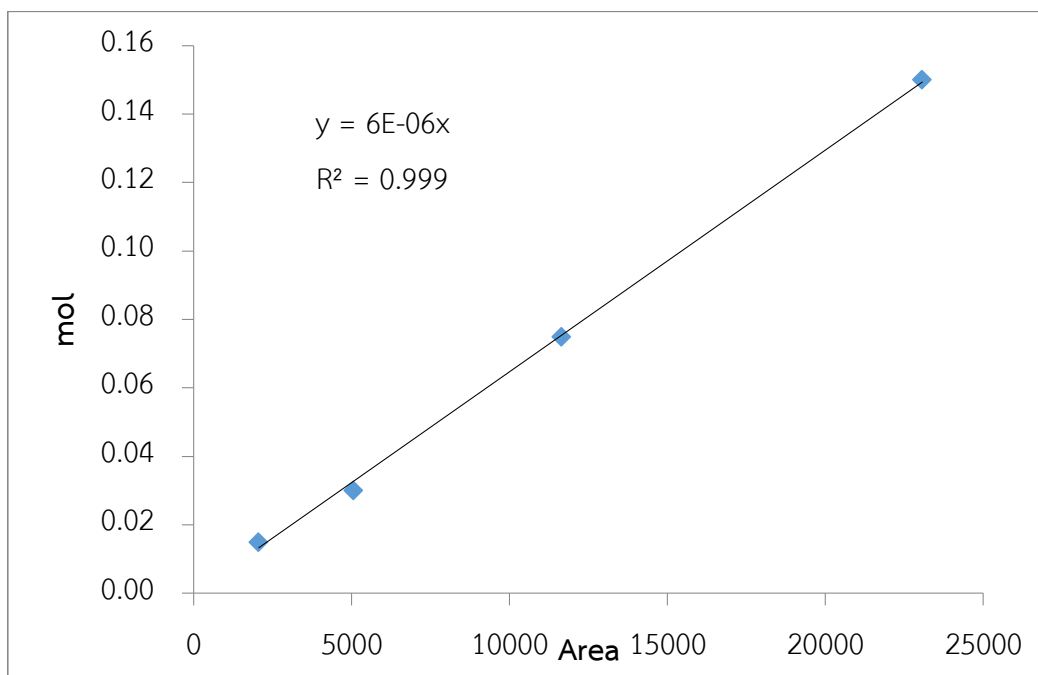


Figure A.4 Calibration curve of Ethanol

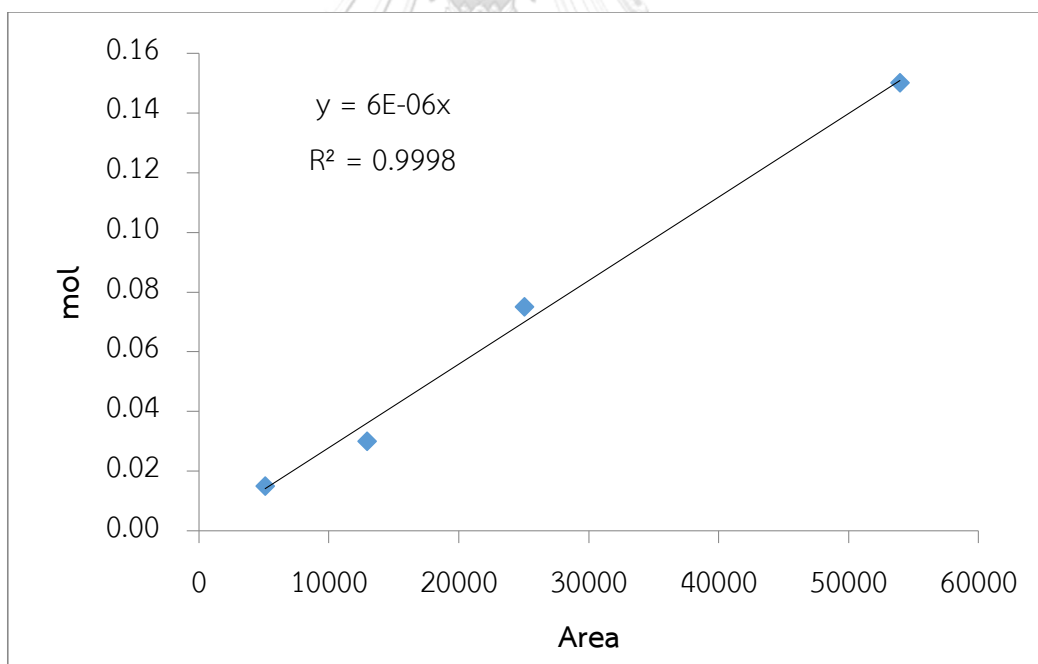


Figure A.5 Calibration curve of n-propanol

APPENDIX B

CALCULATIONS

B.1 Calculation for the preparation of metal oxide loading support (8 wt% WO_x)

Example calculation for the preparation of WO_x/γ-Al₂O₃

Data for calculation:

Mw. of Ammonium (Meta) tungstate ((NH₄)₆H₂W₁₂O₄₀ • H₂O) = 2956.3 g/mole (99.99%)

Preparation 8%wt WO_x/ALOOH catalyst

Based on 100 g of catalyst used, the composition of the catalyst is follow;

Tungsten = 8 g

boehmite (ALOOH) = 100 - 8 = 92 g

For 10 g of ALOOH support used

Tungsten required = $8 \times (10/92) = 0.869$ g

Tungsten 0.869 g was acquired from (NH₄)₆H₂W₁₂O₄₀ • H₂O, which has 99.99% of W basis

Thus, from the AMT give W = $183.84 \times 2 \times 0.9999 = 2205.8$ g

So W 0.869 g required = $0.869 \times (2956.3/2205.8) = 1.165$ g

B.2 Calculation for the preparation of metal loading catalyst (2 wt% Pt)

Example calculation for the preparation of Pt/WO_x/γ-Al₂O₃

Data for calculation:

Mw. of Chloroplatinic acid hydrate (H₂Cl₆Pt • xH₂O) = 409.81 g/mole (38% Pt basis)

Mw of Platinum = 195.084 g/mole

Preparation platinum stock 20%wt/wt

1g of chloroplatinic acid hydrate was dissolved with 4ml of deionized water to design concentration stock.

Preparation 2%wt Pt/WO_x/γ-Al₂O₃ catalyst

Based on 100 g of catalyst used, the composition of the catalyst is follow;

Platinum metal (Pt) = 2 g

Al₂O₃ = 100 - 2 = 98 g

For 1 g of Al₂O₃ support used

Platinum metal required = $1 \times (2/98) = 0.02$ g

Platinum metal 0.00301 g was acquired from H₂Cl₆Pt • xH₂O, which has 38% of Pt basis

H₂Cl₆Pt • xH₂O required = $0.02/0.38 = 0.00537$ g

Thus, from the Pt stock solution with concentration 20%wt/wt

Pt stock solution required = $0.00537 \times (100/20) = 0.02685$ g

The 0.02685 g of Pt stock solution is dissolved in de-ionized water to obtain a suitable amount of aqueous solution for support

APPENDIX C

CALCULATION FOR CO CHEMISORPTION

CO pulse chemisorption was employed to determine the metal active sites on the Pt/WO_x/γ-Al₂O₃ catalyst.

The reaction stoichiometry of CO : Pt = 1 : 1

Let

Weight of catalyst used	= W	g
Peak area of CO per syringe	= A	unit
Integral adsorbed area of CO	= B	unit
Adsorbed ratio	= B/A	unit
Adsorbed quantity per 1 syringe	= 20 × B/A	μL
Volume of CO 1mole of CO at 30°	= 24.85 × 10 ⁶	μL
Mole of adsorbed CO on catalyst	= 20 × (B/A) / 24.85 × 10 ⁶	mmol
Molecule of adsorbed CO on catalyst	= [20 × (B/A) / 24.85 × 10 ⁶] × 6.02 × 10 ²³	molecule
Molecule of adsorbed CO per g-cat.	= [(B/A) × 4.845 × 10 ²³] / W	molecule/g-cat
Amount of metal active site	= Molecule of CO adsorbed per g-cat.	

APPENDIX D

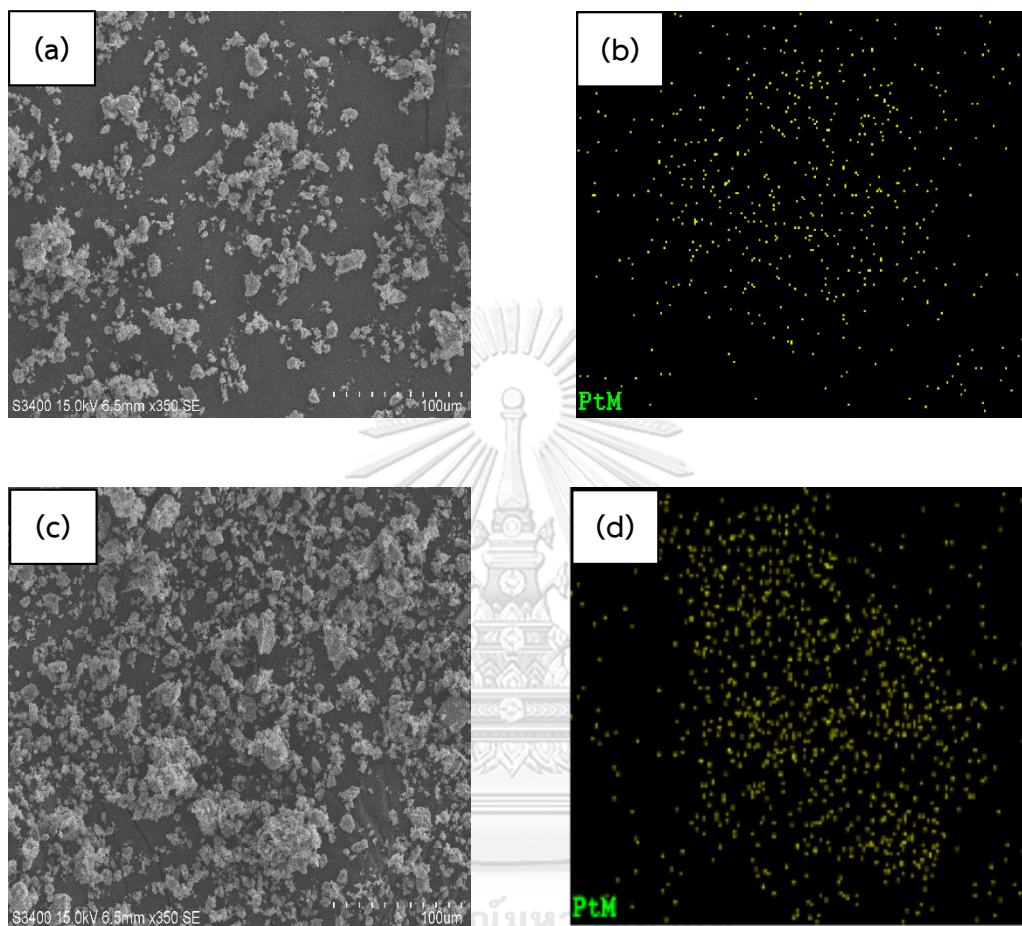
SEM IMAGES AND EDX MAPS FOR Pt/WO_x/γ-Al₂O₃ CATALYSTS

Figure D.1 SEM-EDX for Pt images of (a,b) 5%Pt/WO_x/γ-Al₂O₃ and (c,d) 5%Pt/WO_x/γ-Al₂O₃

APPENDIX E

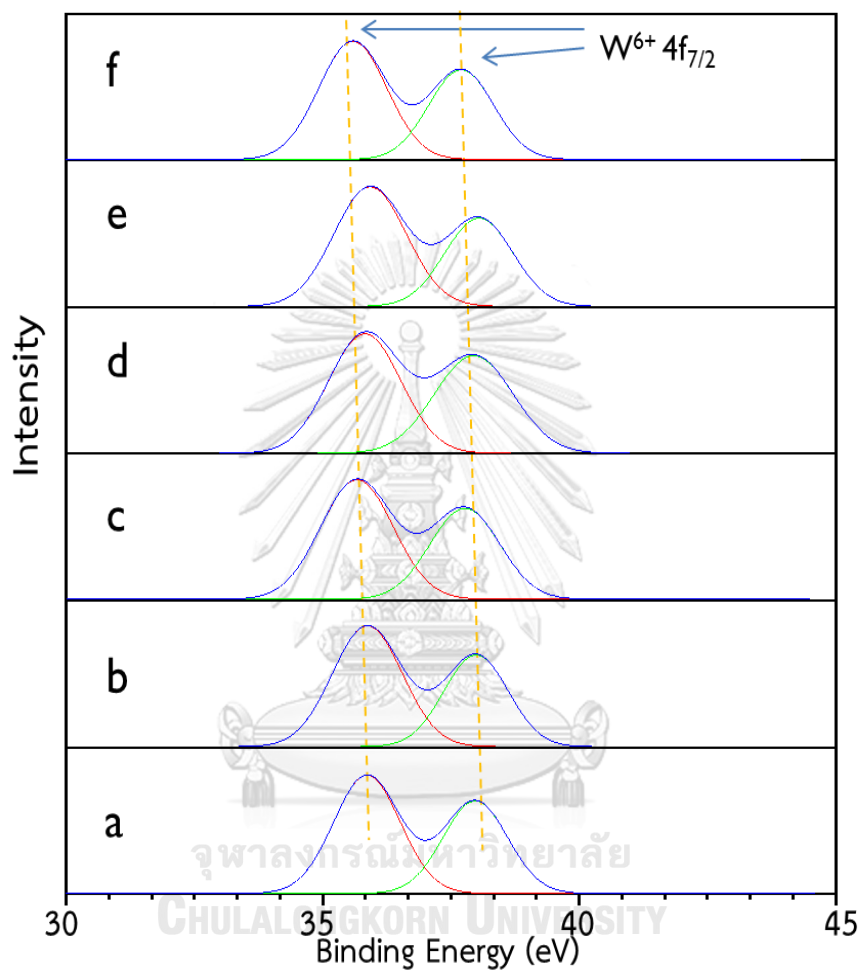
XPS PHOTOEMISSION FOR 2%Pt/WO_x/ALOOH and 2%Pt/WO_x/γ-Al₂O₃

Figure E.1 W 4f XPS spectra of a) 2%Pt/WO_x/ALOOH fresh catalyst, b) 2%Pt/WO_x/ALOOH used, c) 2%Pt/WO_x/ALOOH reduced, d) 2%Pt/WO_x/γ-Al₂O₃ fresh, e) 2%Pt/WO_x/γ-Al₂O₃ used, f) 2%Pt/WO_x/γ-Al₂O₃ reduced.

VITA

NAME	Parama Uttraporn
DATE OF BIRTH	21 July 1993
PLACE OF BIRTH	Songkhla
HOME ADDRESS	64/185 Borommaratchachonnani Road Khet Taling Chan Bang Ramat 10170



จุฬาลงกรณ์มหาวิทยาลัย
CHULALONGKORN UNIVERSITY